

# Twenty Years of Auxiliary-Field Quantum Monte Carlo in Quantum Chemistry: An Overview and Assessment on Main Group Chemistry and Bond-Breaking

Joonho Lee,<sup>1,\*</sup> Hung Q. Pham,<sup>1</sup> and David R. Reichman<sup>1</sup>

<sup>1</sup>*Department of Chemistry, Columbia University, 3000 Broadway, New York, NY, 10027*

In this work, we present an overview of the phaseless auxiliary-field quantum Monte Carlo (ph-AFQMC) approach from a computational quantum chemistry perspective, and present a numerical assessment of its performance on main group chemistry and bond-breaking problems with a total of 1004 relative energies. While our benchmark study is somewhat limited, we make recommendations for the use of ph-AFQMC for general main-group chemistry applications. For systems where single determinant wave functions are qualitatively accurate, we expect the accuracy of ph-AFQMC in conjunction with a single determinant trial wave function to be between that of coupled-cluster with singles and doubles (CCSD) and CCSD with perturbative triples (CCSD(T)). For these applications, ph-AFQMC should be a method of choice when canonical CCSD(T) is too expensive to run. For systems where multi-reference (MR) wave functions are needed for qualitative accuracy, ph-AFQMC is far more accurate than MR perturbation theory methods and competitive with MR configuration interaction (MRCI) methods. Due to the computational efficiency of ph-AFQMC compared to MRCI, we recommended ph-AFQMC as a method of choice for handling dynamic correlation in MR problems. We conclude with a discussion of important directions for future development of the ph-AFQMC approach.

## I. INTRODUCTION

As computational power grows and theoretical algorithms have improved, the importance of the role played by electronic structure theory in chemistry, physics and biology has increased dramatically.<sup>1</sup> For a number of important applications, the predictive power of quantum chemistry has reached the level of “chemical accuracy,” namely relative errors of one kcal/mol.<sup>2</sup> However the most accurate methods are generally the most computationally expensive, and for systems with many electrons, often one must resort to approaches where convergence to predictive accuracy is far from guaranteed. When “gold-standard” wave function-based approaches are impractical, Kohn-Sham density functional theory (DFT) has been the method of choice, due to its combination of accuracy and mild scaling with system size. However, there are many variants of DFT which depend on the choice of functional and it can be difficult *a priori* to select the most accurate density functional for a given application. In addition, DFT generally suffers from self-interaction errors and has difficulty in the treatment of the effects of strong static correlation prevalent in the breaking of chemical bonds and in the electronic structure of transition metal-containing systems.<sup>3</sup> Indeed, even more expensive wave function approaches such as coupled-cluster theory<sup>4</sup> can have difficulty accurately describing strongly correlated cases. Clearly there is still room for the development of novel methods in quantum chemistry which have a high ratio of accuracy to expense and may be reliably applied to challenging chemical problems.

Since the viability of an electronic structure method depends critically on the trade-off between accuracy and scaling with respect to system size, the development of new techniques that push the envelope of accuracy *and* scalability is the primary goal of the field. Adoption of

a method by the community cannot occur before careful and extensive benchmark studies are carried out to establish the domain of validity as well as the benefits and drawbacks of the method in question. It is our aim here to review the foundations of one particularly promising electronic structure framework, namely the auxiliary-field quantum Monte Carlo (AFQMC) approach, and to present, for the first time, the performance of this approach on a large-scale chemical benchmark set.

Unlike DFT or conventional wave function methods, AFQMC employs a statistical as opposed to deterministic route to calculating electronic structure. This necessitates consideration of an entirely different approach to the extraction of ground state energies, and requires the consideration of the role played by statistical fluctuations and error in the solution of the Schrödinger equation. The use and development of AFQMC has notably accelerated in recent years due to new algorithmic advances<sup>5–9</sup> and the publication of promising results on non-trivial chemical problems.<sup>10–17</sup> Unlike standard DFT approaches, AFQMC is free of self-interaction error<sup>16</sup> (as it is a wavefunction method) and is often capable of describing strong correlation effects,<sup>9,18–31</sup> although our focus is not limited to such problems in this work.

AFQMC has its roots in the determinant QMC (DQMC) method proposed by Blankenbecler, Scalapino, and Sugar.<sup>32</sup> DQMC is an exact, unbiased technique, initially developed to describe interacting bosons and fermions at finite temperatures in lattice field theory models of high energy physics. Since its invention, DQMC has been applied to numerous condensed matter problems, most notably the Hubbard model.<sup>33</sup> More recently this approach has been applied to more realistic chemical systems with long-ranged interactions.<sup>34–37</sup> As is the case for DQMC, the scalability of AFQMC is limited by the fermionic sign problem, rendering exact, brute force applications to large chemical systems com-

putationally infeasible.<sup>38</sup> To be more precise, the sign problem manifests in the following way: Per statistical sample, the complexity of the calculation scales polynomially with system size. However, the sample complexity (i.e., the number of statistical samples required for a fixed statistical error) scales exponentially with system size, rendering practical calculations impossible.

To remedy this fundamental barrier in DQMC, Fahy and Hamann proposed the approximate positive projection method,<sup>39</sup> which imposes a constraint to control the sign problem, resembling the fixed-node approximations used in Green’s function Monte Carlo (GFMC)<sup>40,41</sup> and diffusion Monte Carlo (DMC).<sup>42</sup> Adopting this approximation for open-ended random walks, Zhang, Carlson, and Gubernatis<sup>43</sup> proposed the constrained path approximation, and this method will be referred to as cp-AFQMC. cp-AFQMC has been successfully applied to non-trivial electronic lattice problems,<sup>44–61</sup> bosonic lattice problems,<sup>62,63</sup> and mixed fermions-bosons systems.<sup>64,65</sup> cp-AFQMC has been shown to be one of the more accurate and scalable many-body methods in numerous benchmark studies,<sup>49,57,58</sup> although it is important to bear in mind that like all constrained quantum Monte Carlo methods, cp-AFQMC is approximate and its domain of validity has not been fully mapped out.

The generalization of cp-AFQMC to chemical systems with long-range interactions yields the phaseless AFQMC (ph-AFQMC) which is the focus of this work.<sup>66</sup> Since its invention by Zhang and Krakauer in 2003,<sup>66</sup> ph-AFQMC has gained popularity in the quantum chemistry community due to its relative computational affordability and its accuracy, as demonstrated in recent calculations including those performed on small but challenging molecular systems,<sup>9,18–31</sup> simple transition metal complexes,<sup>10–17</sup> and solids.<sup>5,67–80</sup> ph-AFQMC is highly flexible in that the accuracy of the approach may be systematically improved by the use of increasingly sophisticated trial wave functions. In addition, ph-AFQMC has become more accessible to users via the development of open-source codes.<sup>81–83</sup>

Despite its growing usage in the chemistry community, it is not clear how well ph-AFQMC performs for a wide range of main group chemistry applications. While it has been speculated that ph-AFQMC with the simplest form of a single-reference trial wave function has an accuracy on par with coupled-cluster with singles, doubles, and perturbative triples (CCSD(T)),<sup>18,31,73,84</sup> there has been no extensive body of work that confirms this expectation. While ph-AFQMC has been compared to other commonly used quantum chemistry methods such as CCSD(T) on simple bond breaking problems such as those that occur in H<sub>2</sub>O,<sup>18</sup> BH,<sup>21</sup> N<sub>2</sub>,<sup>21</sup> F<sub>2</sub>,<sup>23</sup> C<sub>2</sub>,<sup>22</sup> Cr<sub>2</sub>,<sup>11</sup> and Mo<sub>2</sub>,<sup>12</sup> studies comparing ph-AFQMC with both single-reference CCSD(T) and other multi-reference methods have been relatively scarce. Given the accuracy of ph-AFQMC for dynamic correlation problems,<sup>15,31,69,75</sup> it is crucial to compare its accuracy with other multi-reference dynamic correlation methods,

such as perturbation theory and configuration interaction methods.

The goal of this manuscript is both to present a pedagogical review of ph-AFQMC from the quantum chemistry perspective as well as to investigate the performance of ph-AFQMC on a large chemical benchmark series, namely a thermochemistry benchmark set (W4-11),<sup>85</sup> a non-covalent interaction benchmark set (A24),<sup>86</sup> and model molecular bond dissociation problems (H<sub>4</sub> and N<sub>2</sub>).<sup>87–95</sup> From this, we hope to establish fair expectations for ph-AFQMC for main group chemistry and simple strong correlation problems associated with the breaking of chemical bonds, and to further encourage the use and development of ph-AFQMC in quantum chemistry in the future. We note that there exist other pedagogical reviews written from a somewhat different perspective<sup>96–98</sup> which the interested reader is encouraged to consult.

It should be noted that the applications considered here, while chemically important, are somewhat uncommon for ph-AFQMC. In particular, the benchmark sets (W4-11<sup>85</sup> and A24<sup>86</sup>) considered here are predominantly single reference problems. These do not involve strong electron correlation for which ph-AFQMC has been frequently used. Indeed, these benchmark problems are already known to be well-characterized by coupled-cluster techniques. Furthermore, we mostly consider the *least* accurate and the most efficient variant of ph-AFQMC. Namely we employ a simple single-determinant trial wave function, although we do discuss selected examples where the use of multi-determinant trials can greatly improve accuracy. These choices are purposeful ones: we aim to assess the breadth and baseline accuracy of the approach in situations where other quantum chemistry methods such as CCSD(T) are often well-suited. The main points that we will deliver in this manuscript are as follows:

1. For main group chemistry applications, with  $\mathcal{O}(N^3) - \mathcal{O}(N^4)$  scaling per sample, ph-AFQMC with a single-reference trial wave function is more accurate than CCSD ( $\mathcal{O}(N^6)$ ) and is competitive with, albeit somewhat less accurate, than CCSD(T) ( $\mathcal{O}(N^7)$ ) and state-of-the-art density functionals.
2. For bond breaking, while maintaining  $\mathcal{O}(N^3) - \mathcal{O}(N^4)$  scaling per sample, the accuracy of ph-AFQMC with a multi-reference trial wave function surpasses that of low-order multi-reference perturbation theory ( $\mathcal{O}(N^5) - \mathcal{O}(N^6)$ ) and is comparable in accuracy with multi-reference configuration interaction methods ( $\mathcal{O}(N^6)$ ).
3. Given the relatively short history of ph-AFQMC in quantum chemistry, many aspects of the algorithm deserve further investigation and there is much room for improvements to the current implementation of the approach. We will conclude this work with a discussion of these opportunities.

This manuscript is organized as follows: In Section II we present an overview of the AFQMC method and its phaseless variant (ph-AFQMC). A discussion of trial wave functions, the calculation of observables, size-consistency and computational cost is contained in this section. In Section III we present benchmark results with a comparison with other approaches. Section IV presents a discussion of lessons learned from our calculations and prospects for future development. We conclude in Section V. The Appendices contain details omitted from the main text.

## II. OVERVIEW OF PHASELESS AUXILIARY-FIELD QUANTUM MONTE CARLO

### A. Ground-state calculations

We refer the interested readers to Appendix A0 A1 for a more detailed formal exposition of AFQMC. Here, we focus on a short summary of the methodology. We assume the spin-orbital notation throughout this paper.

AFQMC is what is called a “projector” QMC algorithm because it projects towards the ground state from an initial wave function which has a non-zero overlap with the true, exact ground state of the system. Formally, the ground-state wave function  $|\Psi_0\rangle$  of a Hamiltonian  $\hat{H}$  is found by via imaginary time propagation

$$|\Psi_0\rangle = \lim_{\tau \rightarrow \infty} e^{-\tau \hat{H}} |\Phi_0\rangle, \quad (1)$$

where  $\hat{H}$  is an *ab initio* Hamiltonian,

$$\hat{H} = \sum_{pq} h_{pq} a_p^\dagger a_q + \frac{1}{2} \sum_{pqrs} (pr|qs) a_p^\dagger a_q^\dagger a_s a_r, \quad (2)$$

$\tau$  is the imaginary time, and  $|\Phi_0\rangle$  is an initial wave function that is not orthogonal to  $|\Psi_0\rangle$ . The form of  $|\Psi_0\rangle$  in Eq. (1) resembles the CCSD wave function with generalized singles and doubles,<sup>99,100</sup> but in AFQMC there is no cluster amplitude to be determined, and formally Eq. (1) is exact.

Discretizing  $\tau$  and applying the Trotter decomposition<sup>101</sup> followed by the Hubbard-Stratonovich (HS)<sup>102</sup> transformation to the propagator  $e^{-\Delta\tau \hat{H}}$ , one obtains a high-dimensional integral formula for the imaginary time evolution operator over a short time interval

$$e^{-\Delta\tau \hat{H}} = \int d^{N_\gamma} \mathbf{x} p(\mathbf{x}) \hat{B}(\mathbf{x}) + \mathcal{O}(\Delta\tau^2), \quad (3)$$

where  $\Delta\tau$  is the infinitesimal time step,  $p(\mathbf{x})$  is the standard normal distribution and  $\hat{B}(\mathbf{x})$  is an effective one-body propagator that is obtained from one-body operators coupled to  $\mathbf{x}$ , a vector of  $N_\gamma$  classical auxiliary fields. Since only one-body operators now appear, this representation of the short-time propagator is often viewed as the exact mapping of an interacting many-body system to an

ensemble of non-interacting systems, each coupled to a classical, fluctuating external potential. The many-body correlation beyond mean-field theory is recovered upon the integration over the auxiliary fields.

The phaseless AFQMC (ph-AFQMC)<sup>66</sup> approach utilizes importance sampling based on a trial wave function  $|\Psi_T\rangle$  during the random walk process. To carry this out, one writes the global wave function at time  $\tau$  as a weighted statistical sum over  $N_{\text{walkers}}$  “walkers”,

$$|\Psi(\tau)\rangle = \sum_{i=1}^{N_{\text{walkers}}} w_i(\tau) \frac{|\psi_i(\tau)\rangle}{\langle \Psi_T | \psi_i(\tau) \rangle}. \quad (4)$$

Given this importance sampling, the walker weight update rule follows

$$w_i(\tau + \Delta\tau) = w_i(\tau) \times S(\mathbf{x}_i(\tau), |\psi_i(\tau)\rangle), \quad (5)$$

where the overlap ratio  $S$  is given by

$$S(\mathbf{x}_i(\tau), |\psi_i(\tau)\rangle) = \frac{\langle \Psi_T | \hat{B}(\mathbf{x}_i(\tau)) | \psi_i(\tau) \rangle}{\langle \Psi_T | \psi_i(\tau) \rangle}. \quad (6)$$

Since this weight update rule cannot guarantee that the walker weights are real and positive,  $\{w_i\}$ , Eq. (5) leads to the fermionic phase (sign) problem with a diverging variance for any observable when calculated by the protocol outlined below.<sup>38</sup>

To control the phase problem, ph-AFQMC imposes a constraint to ensure the positivity of the weights throughout the imaginary time propagation. The constraint that defines the standard ph-AFQMC approach is given by a modified overlap ratio,  $S_{\text{ph}}$ ,

$$S_{\text{ph}}(\mathbf{x}_i(\tau), |\psi_i(\tau)\rangle) = \|S(\mathbf{x}_i(\tau)|\psi_i(\tau))\| \times \max(0, \cos \theta_i(\tau)), \quad (7)$$

where the phase  $\theta_i(\tau)$  is given by

$$\theta_i(\tau) = \arg S(\mathbf{x}_i(\tau)|\psi_i(\tau)). \quad (8)$$

This modified overlap ratio is used in ph-AFQMC to update the weights. It should be emphasized that this constrained random walk introduces systematic biases which induce deviations in the values of observables (such as the ground state energy) compared to the exact values. It should be noted that this bias disappears in the limit of  $|\Psi_T\rangle$  becoming an exact eigenstate of  $\hat{H}$ . This fact introduces a means to improve the accuracy of ph-AFQMC by increasing the sophistication of the trial function  $|\Psi_T\rangle$ . We will return to this point later in this work. A different way to view the constraint is that one imposes a gauge boundary condition (i.e., a global phase) for the wave function sampled through the imaginary time evolution.

Within this framework, the global energy estimate at a given imaginary time  $\tau$  is given by a weighted statistical average,

$$\langle O(\tau) \rangle_{\text{mixed}} = \frac{\sum_i w_i(\tau) O_{L,i}(\tau)}{\sum_i w_i(\tau)}, \quad (9)$$

where the local estimate for observable  $\hat{O}$  of the  $i$ -th walker is given by

$$O_{L,i}(\tau) = \frac{\langle \Psi_T | \hat{O} | \psi_i(\tau) \rangle}{\langle \Psi_T | \psi_i(\tau) \rangle}. \quad (10)$$

If  $\hat{O} = \hat{H}$ , these estimates are global energy and local energy estimates, respectively. Given the positivity of  $\{w_i\}$ , the variance of this energy estimate grows linearly with system size, ensuring the polynomial-scaling sample complexity of the overall algorithm. It is important to remark here that the resulting ph-AFQMC energy computed via Eq. (9) is not guaranteed to be variational.<sup>103</sup>

## B. Trial wave functions

The accuracy of ph-AFQMC heavily depends on the quality of the trial wave function employed in the calculation. Conceptually, the role played by the trial wave function is very different from that of the reference wave function used in conventional quantum chemistry methods such as CCSD(T). Despite this difference, it is convenient to think of ph-AFQMC as adding correlation energy on top of an *a priori* chosen trial wave function. Here, we summarize existing strategies for generating these ph-AFQMC trial states.

Single determinant (SD) trial wave functions are the most widely used and they offer the most affordable variant of the ph-AFQMC algorithm. There are multiple approaches to obtain single determinant trial wave functions. One way is to employ the lowest energy spin-unrestricted or spin-generalized Hartree-Fock (HF) wave function.<sup>16,30</sup> This approach can be well-suited for describing bond dissociation as shown in Section III C. While this approach is completely parameter-free, it often runs into issues associated with artificial symmetry breaking.<sup>16,104</sup> In particular, HF wave functions can exhibit an unphysical breaking of symmetry that makes post-HF calculations behave erratically in energetics and properties.<sup>105–112</sup> While ph-AFQMC can correct artificial symmetry breaking to some extent through imaginary time evolution, there are cases where the lowest energy HF solution is clearly not the best SD trial wave function.<sup>16</sup> Alternatively, one can obtain a single Slater determinant from methods that include electron correlation effects. For this, DFT<sup>10,66</sup> and regularized orbital optimized Møller-Plesset perturbation theory (OOMP2) have been used.<sup>16,113</sup> More broadly, one can employ any approximate Brueckner orbital wave functions<sup>114,115</sup> for this purpose. We also note that the recently-defined self-consistent trial wave function method<sup>98,116</sup> also fits into the category of an SD trial wave function approach.

More elaborate trial wave functions may be used within ph-AFQMC, which confer greater accuracy for a greater computational expense. Most commonly, a linear combination of SDs, often referred to as multi-Slater determinants or MSDs for short, are employed.<sup>9,21,23,30</sup> The

MSD trial can be obtained from a truncated configuration interaction (CI) expansion, complete active space CI (CASCI), or from selected CI methods.<sup>117</sup> While these trial wave functions can yield excellent ph-AFQMC energies, they are brute-force in nature and the cost of obtaining these trial wave functions generally scales exponentially with system size, which can limit the applicability of their use within ph-AFQMC.

Lastly, there are non-linear trial wave functions which may be used. These include Jastrow factors,<sup>51,118</sup> coupled-cluster wave functions,<sup>4,37,119</sup> perfect-pairing wave functions,<sup>23,119,120</sup> and transcorrelated wave functions.<sup>121</sup> The cost of obtaining these wave functions in all such cases is polynomial-scaling, which makes them appealing for use as trials. Furthermore, these wave functions approximate the exact ground state much more accurately than do SD trial functions as they all include electron correlation inherently missing from the SD description. Unfortunately, using these non-linear wave function as a trial wave functions without any approximations is currently extremely difficult on both classical and quantum computing platforms.<sup>119</sup> The efficient and accurate use of such trial states within ph-AFQMC will require further work to become viable.

## C. Physical properties extracted from ph-AFQMC

In practical applications, one may want to evaluate observables that do not commute with  $\hat{H}$ . Most commonly, these observables are associated directly with reduced density matrices (RDMs) or some elements of them. The computation of such observables introduces additional challenges within the ph-AFQMC framework, because the mixed estimator in Eq. (9) is no longer unbiased. For such quantities, we need to use a different estimator known as the “pure” estimator. This problem is analogous to the issues associated with coupled-cluster expectation values<sup>122</sup> which are typically now handled by the coupled-cluster Lagrangian formalism.<sup>123</sup>

A computationally simple approach to this problem is to use the approximate variational estimator

$$\langle O(\tau) \rangle_{\text{pure}} \approx 2 \langle O(\tau) \rangle_{\text{mixed}} - \frac{\langle \Psi_T | \hat{O} | \Psi_T \rangle}{\langle \Psi_T | \Psi_T \rangle}, \quad (11)$$

which is frequently used in diffusion Monte Carlo.<sup>124,125</sup> Recently, Eq. (11) was used within the ph-AFQMC framework to estimate the dipole moments of simple molecules.<sup>9</sup> Here, it was found that the quality of the trial wave function is critically important for accurately approximating the pure estimates. For this quantity, using SD trial wave functions yielded very inaccurate results for the systems considered in Ref. 9.

Another approach that is more commonly used in ph-AFQMC calculations is the back-propagation algorithm.<sup>25,62,126</sup> Here, one propagates the bra state ( $\langle \Psi_T |$ ) in the mixed estimator (Eq. (A10)) backward in time

such that the resulting estimator is symmetric with respect to both the bra and ket, ultimately resembling the pure (or variational) estimator. Formally, this entails computing observables using the following estimate:

$$\begin{aligned} \langle O(\tau) \rangle_{\text{pure}} &\approx \lim_{\kappa \rightarrow \infty} \frac{\langle \Psi_T | e^{-\kappa \hat{H}} \hat{O} | \Psi(\tau) \rangle}{\langle \Psi_T | e^{-\kappa \hat{H}} | \Psi(\tau) \rangle} \\ &= \lim_{\kappa \rightarrow \infty} \frac{\sum_i w_i(\tau + \kappa) \frac{\langle \psi_i(\kappa) | \hat{O} | \psi_i(\tau) \rangle}{\langle \psi_i(\kappa) | \psi_i(\tau) \rangle}}{\sum_i w_i(\tau + \kappa)}, \end{aligned} \quad (12)$$

where the back-propagation time,  $\kappa$ , while formally taken to  $\infty$ , is in practice fixed to a long enough finite time length. This approach is computationally efficient, but its accuracy for at least some *ab initio* systems has been shown to be rather poor.<sup>25,80</sup> There are additional algorithmic ways to reduce the back-propagation bias, such as partially restoring the phase and cosine factors along the back propagation portion of the path.<sup>25,98</sup> However, even with these considerations, the resulting 1-RDMs were found to be inaccurate, at least in some systems.<sup>80</sup> Devising improved algorithms for accurately computing pure estimates for observables without greatly increasing the computational cost of the calculations is a worthy goal for future research.

#### D. Size-consistency

Size-consistency is a property of a wave function for isolated systems  $A$  and  $B$  that guarantees the product separability of a supersystem wave function ( $|\Psi_{AB}\rangle = |\Psi_A\rangle|\Psi_B\rangle$ ) as well as the additive separability of energy ( $E_{AB} = E_A + E_B$ ).<sup>127</sup> This property has important implications concerning the applicability of a given method to large systems and is therefore considered to be an important formal property in method development. The size-consistency of ph-AFQMC was first examined in Ref. 73, but some subtle issues were not fully discussed in that work. Here, we will provide the first rigorous analysis of size-consistency within ph-AFQMC.

We will assume that the trial wave function is product separable, and that for isolated systems  $A$  and  $B$ , the total Hamiltonian separates into  $\hat{H}_A$  and  $\hat{H}_B$  which commute with each other. Given these conditions, the propagator is product separable,

$$\exp(-\Delta\tau \hat{H}_{AB}) = \exp(-\Delta\tau \hat{H}_A) \exp(-\Delta\tau \hat{H}_B), \quad (13)$$

which leads to the product separability of  $\hat{B}$ ,  $\hat{B}_{AB} = \hat{B}_A \hat{B}_B$ .

Provided that the walker wave function is product separable, it can be shown that the overlap ratio in Eq. (6) of the total system,  $S^{AB}$ , is product separable into monomer overlap ratios,  $S^A$  and  $S^B$

$$S^{AB} = \frac{\langle \Psi_T^A | \hat{B}_A | \psi^A \rangle \langle \Psi_T^B | \hat{B}_B | \psi^B \rangle}{\langle \Psi_T | \psi^A \rangle \langle \Psi_T | \psi^B \rangle} = S^A S^B. \quad (14)$$

The product separability of the walker wave function can be satisfied as long as we start from a product separable wave function since the propagator itself is product separable. With this overlap ratio, walker weights are also product separable as  $w^{AB} = w^A w^B$ . Since the local energy in Eq. (10) is additively separable ( $E_f^{AB} = E_f^A + E_f^B$ ), we conclude that  $\langle E^{AB} \rangle = \langle E^A \rangle + \langle E^B \rangle$ .

However, the above analysis does not apply to the modified overlap ratio for arbitrary imaginary time steps in Eq. (7) used in the constrained ph-AFQMC formalism. To see this, noting the cosine projection which defines the constraint for the ph-AFQMC framework, we have

$$\exp(i\theta^{AB}) = \exp(i\theta^A) \exp(i\theta^B) \quad (15)$$

$$\cos(\theta^A + \theta^B) = \cos(\theta^A) \cos(\theta^B) - \sin(\theta^A) \sin(\theta^B), \quad (16)$$

where the cosine factor is not product separable, leading to size-inconsistency in the overall approach if the time step is not taken to zero. In other words, the walker weights of the total system are not product separable ( $w^{AB} \neq w^A w^B$ ). The magnitude of the size-inconsistency error is proportional to the magnitude of the sine terms in Eq. (16), and can be practically small. Importantly, if the time step  $\Delta t$  is small, then  $\theta^A$  and  $\theta^B$  are small. Therefore, we expect the size-inconsistency error to vanish in the limit of  $\Delta t \rightarrow 0$ . We present numerical results to support this in Appendix A0 A2. In this sense, the size-inconsistency error is a part of the time step error with an  $\mathcal{O}(\Delta t)$  error scaling as opposed to  $\mathcal{O}(\Delta t^2)$  of the Trotter error. Like other time step errors, the above analysis suggests that size-inconsistency error can be controlled within ph-AFQMC by taking the limit of  $\Delta t \rightarrow 0$ . While we examined the size-consistency of ph-AFQMC assuming localized orbitals and product-separability of the trial wavefunction, it is possible that these assumptions may not be necessary to examine the size-consistency more generally.

In summary, we have shown that ph-AFQMC is strictly size-consistent in the limit of  $\Delta t \rightarrow 0$ . The size-consistency is critically important to reliably apply ph-AFQMC to large systems and solid state problems, similarly to more traditional quantum chemistry methods such as coupled-cluster theory.

#### E. Computational cost

The computational expense and scaling with system size of ph-AFQMC is an important factor when considering suitable applications for this approach. The integral transform often necessary for ph-AFQMC scales as  $\mathcal{O}(N^4)$ . There are three additional considerations that need to be considered within ph-AFQMC to determine the scaling behavior and how it depends on the choice of a trial wave function. For the following discussion, we will assume that the walker wave functions are SDs. The first consideration concerns the propagation step. The central quantity to be computed is the modified overlap

	SD	MSD	Non-linear
$\langle \Psi_T   \psi_i(\tau) \rangle$	$\mathcal{O}(N^3)$	$\mathcal{O}(N_c + N^3)^{37}$	$\mathcal{O}(e^N)$
Green’s function	$\mathcal{O}(N^3)$	$\mathcal{O}(N_c + N^3)^9$	$\mathcal{O}(e^N)$
Local energy	$\mathcal{O}(N^4)$ $\mathcal{O}(N^3)$	$\mathcal{O}(N_c N + N^4)^{37}$ $\mathcal{O}(N_c N^2 + N^3)^8$	$\mathcal{O}(e^N)$

TABLE I. Summary of ph-AFQMC per-sample costs of each component (overlap, one-body Green’s function (see Eq. (A14)), and local energy (see Eq. (10))) for single-determinant (SD), multi Slater determinant (MSD), and non-linear trial wave functions.  $N$  denotes system size and  $N_c$  is the number of determinants in an MSD trial wave function. The cubic-scaling for the local energy evaluation in the case of SD follows from arguments presented in Refs. 5–8.

ratio in Eq. (7). Specifically, the overlap between the trial and walker wave functions,  $\langle \Psi_T | \psi_i(\tau) \rangle$ , must be efficiently evaluated if the method is to be computationally viable. In addition to the overlap, one needs to evaluate the one-body Green’s function for the force bias evaluation (see Appendix A0A1 for more details). The final consideration relates to cost of the local energy evaluation in Eq. (10) assuming that the ground state energy is the quantity of interest. In Table I we summarize the cost of these three parts for different types of trial wave functions discussed in Section IIB.

For the local energy evaluation there has been a variety of recent algorithmic improvements. For example, the best algorithms now available reduce the standard quartic-scaling algorithm of the SD local energy evaluation to a cubic-scaling algorithm. This can be achieved by using double factorization,<sup>6</sup> tensor hypercontraction,<sup>5</sup> stochastic resolution-of-the-identity,<sup>7</sup> or via the use of localized orbitals.<sup>8</sup> Accelerating the local energy evaluation with multi-SD trials has not been explored as extensively as that of the simpler SD case, but recent explorations with localized orbitals<sup>8</sup> and with generalized Wick’s theorem<sup>9,37</sup> are encouraging. Future work should be aimed at lowering the complexity of the overlap and the force bias evaluation since these computations often form the bottleneck for medium-sized molecules.

If one is to compare the cost of standard deterministic quantum chemistry methods to the cost of ph-AFQMC, a subtlety arises due to the statistical nature of ph-AFQMC. For bulk systems when energy per particle or other size-intensive quantities are relevant, our cost analysis given in Table Table I is sufficient, assuming the number of samples required for desired precision does not grow with system size. For finite molecular systems, it is sensible to estimate the cost of ph-AFQMC for a fixed statistical error as the system size,  $N$ , increases. Assuming that the auto-correlation time in the Markov chain does not grow with  $N$  and that the standard error in the energy estimate grows linearly with  $N$ , one crudely requires  $\mathcal{O}(N^2)$  statistical samples to maintain a fixed statistical error. Therefore, we find a  $\mathcal{O}(N^2)$  multiplicative factor in addition to the cost in Table I. While this is a correct formal asymptotic scaling, it is possible

that in practice one may not experience  $\mathcal{O}(N^2)$  sample complexity if the trial wave function is accurate such that the statistical fluctuations are suppressed below a desired error threshold for the range of system sizes under consideration.

### III. PERFORMANCE OF PH-AFQMC FOR THERMOCHEMISTRY AND THE TREATMENT OF NON-COVALENT INTERACTIONS AND BOND DISSOCIATION

We will now assess the accuracy of ph-AFQMC using well-known thermochemistry and non-covalent interaction benchmark sets, along with several simple bond dissociation examples. For simplicity, we will refer to ph-AFQMC as AFQMC in this section. Computational details are available in Appendix A0A3. Note that nearly all of the AFQMC calculations presented here are new and have not been previously published.

#### A. Thermochemistry benchmark (W4-11)

W4-11<sup>85</sup> is a high-quality benchmark set with a total of 979 relative energies. This data set has been extensively used to assess the performance of distinct density functionals<sup>2,128</sup> and other quantum chemical methods.<sup>87–95</sup> It covers a variety of chemical reactions for the main-group elements, including 140 total atomization energies (TAE140), 707 heavy-atom transfer energies (HAT707), 99 bond dissociation energies (BDE99), 20 isomerization energies (ISO20), and 13 nucleophilic substitution reaction energies (SN13). In addition, it is an economical benchmark set because one can generate the remainder of the 839 data points using the TAE140 data, which only requires 152 single point energy calculations.

We note that not every data point in the W4-11 set is a simple single-reference (SR) problem. The TAE140 subset contains 16 multi-reference (MR) data points determined by the %TAE<sub>e</sub>[(T)] diagnostic.<sup>85</sup> Similarly, 202 energies in the HAT707 set and 16 energies in the BDE99 set have also been deemed MR data points.<sup>2</sup> We will discuss the performance of ph-AFQMC on 745 SR data points separately from the 234 MR data points, as is often done for density functionals and other quantum chemistry methods.<sup>2</sup>

##### 1. Single atom total energies

The simplest systems in the W4-11 set are single atoms (Be, B, C, N, O, F, Al, Si, P, S, Cl). These are systems are small enough that brute-force methods such as SHCI can be reliably performed to obtain exact total energies. We first look at the performance of CCSD(T) and AFQMC for these in the aug-cc-pVTZ basis set as shown in Fig. 1. We used spin-restricted open-shell Hartree-Fock (ROHF)

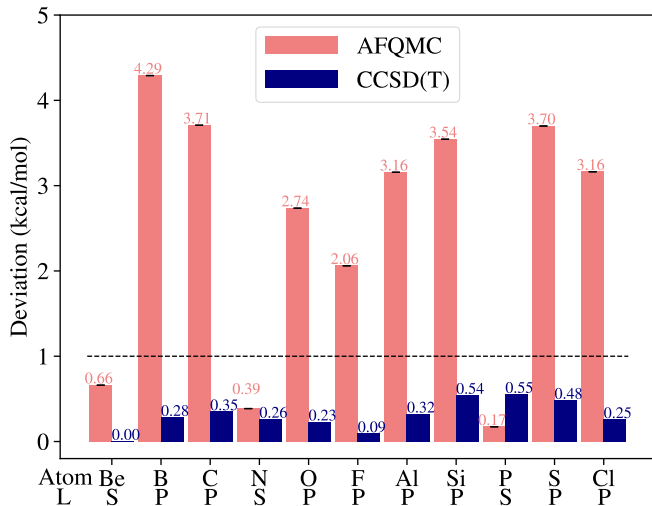


FIG. 1. Deviation (in kcal/mol) of AFQMC (blue) and CCSD(T) (orange) from exact energies in an aug-cc-pVTZ basis. The error bars for AFQMC are nearly undetectable on this energy scale. In the X-axis ticks, we also indicate the angular momentum (L) of the ground state of each atom. The black dotted lines indicate the “chemical accuracy” value of 1 kcal/mol.

as a reference state for CCSD(T) and as a trial state for AFQMC. The conclusions are unchanged if one uses a spin-unrestricted Hartree-Fock (UHF) trial instead.

In Fig. 1, CCSD(T) achieves chemical accuracy (1 kcal/mol) for all the atoms in W4-11. However, AFQMC exhibits large errors above 2 kcal/mol for numerous atoms. There is an interesting trend that the AFQMC error becomes an order of magnitude smaller for atoms whose ground state angular momentum is of S symmetry. For all the other cases (ground state angular momentum, P), AFQMC errors are greater than 2 kcal/mol. We conducted a preliminary investigation of this trend using various different SD and MSD trials with the hypothesis that these large errors can be attributed to simple symmetry constraints, as seen in the Hubbard model.<sup>48,50</sup> Unfortunately, while one can converge all of the atomic energies to chemical accuracy with a sophisticated multi-SD trial, we were unable to find a simple, compact trial wave function that removes this bias. For instance, we investigated C in aug-cc-pVTZ further with an exact trial wavefunction generated by SHCI. To achieve chemical accuracy, we needed more than 200 determinants in the trial wavefunction which has more than 0.99 overlap with the exact ground state.

Very recent work suggests that using SD trial wave functions with a partially relaxed constraint may reduce the bias significantly although the accuracy of such a constraint on large systems remains unclear.<sup>129</sup> Alternatively, one could even perform free-projection<sup>37</sup> or release constraint<sup>48</sup> calculations with SD trial wave functions on these small atoms, but this is not a viable option for larger systems. We leave further investigation

of these simple systems for future studies, and focus on the performance of AFQMC for W4-11 where we use CCSD(T) atomic energies but AFQMC molecular energies. Lastly, we note that due to the frozen core approximation, Be contains only two electrons that need to be correlated. Therefore, CCSD is exact for this system, as shown in Fig. 1. However, this exactness does not apply to AFQMC.

## 2. Single-reference systems

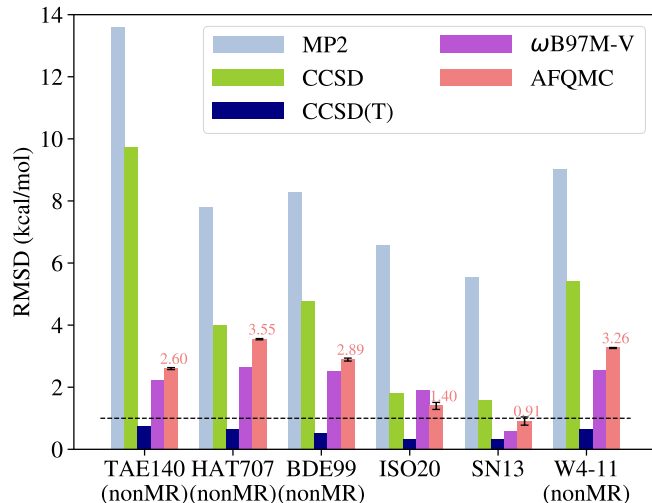


FIG. 2. Root-mean-square deviation (RMSD) for each subset of the W4-11 data set and for the overall W4-11 set, including only nonMR (i.e., SR) data points. The black dotted lines indicate the “chemical accuracy” value of 1 kcal/mol.

We have performed CCSD(T) and AFQMC using both SD RHF and UHF states as references or trial functions, respectively. We report the raw energies of each case in the Zenodo repository.<sup>130</sup> For AFQMC, it was found that the use of UHF trials leads to more accurate results, while for CCSD(T) using an RHF references was statistically superior. Hence, we will compare AFQMC with UHF trials and CCSD(T) with RHF reference for all single-reference calculations.

In Fig. 2, we observe systematic improvements for both the root-mean-square deviation (RMSD) and mean-signed error (MSE) as we increase the sophistication of the correlation treatment, with second-order Møller-Plesset perturbation theory (MP2) less accurate than CCSD which is less accurate than CCSD(T). However, both MP2 (9.01 kcal/mol) and CCSD (5.40 kcal/mol) do not achieve chemical accuracy in terms of RMSD for any of the W4-11 subsets. CCSD(T) achieves chemical accuracy in all subsets of W4-11 (total RMSD = 0.63 kcal/mol). We compare our results against a combinatorially optimized density functional, namely  $\omega$ B97M-V,<sup>131</sup> which was found to be the best functional out of 200 functionals examined in Ref. 2. While there are now even

more accurate functionals (e.g. double hybrid functionals<sup>132,133</sup>), we believe that  $\omega$ B97M-V serves as an example of an accurate functional for the types of systems we investigate here. Data for other functionals are available in Ref. 2.  $\omega$ B97M-V provides chemical accuracy only for the SN13 subset and within the complete W4-11 set its RMSD is 2.52 kcal/mol. AFQMC performs quite similarly to  $\omega$ B97M-V in that it achieves chemical accuracy for the SN13 subset but not for any other subsets. Overall, AFQMC’s RMSD is 3.26 kcal/mol which is slightly worse than  $\omega$ B97M-V. However, we note that this is still an improvement over CCSD (5.40 kcal/mol) by a sizable margin. As the data points in TAE140 completely determine relative energies in all the other subsets, we see qualitatively similar statistical results between the TAE140 subset and the entire W4-11 data set.

### 3. Multi-reference data points

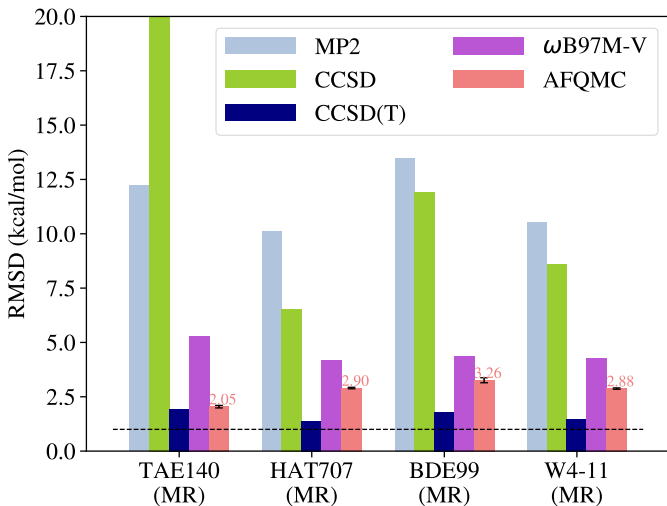


FIG. 3. Root-mean-square deviation (RMSD) (in kcal/mol) for the MR data points in the TAE140, HAT707, and BDE99 subsets of the W4-11 data set, along with the overall aggregate W4-11 MR data points. The black dotted lines indicate the “chemical accuracy” value of 1 kcal/mol.

For 234 MR data points, we performed the same analysis as shown in Fig. 3. With the exception of the error of CCSD for the TAE140 MR set, the relative performance between different methods over MR data points is the same as that over each of the SR data sets and within W4-11 overall. Similarly to the SR case shown in Fig. 2, MP2 (10.51 kcal/mol) and CCSD (8.59 kcal/mol) are found to be significantly less accurate than CCSD(T) overall. CCSD(T) also does not perform as well for these data points, yielding an RMSD of 1.44 kcal/mol.  $\omega$ B97M-V has an RMSD of 4.27 kcal/mol overall for the MR W4-11 data set. AFQMC is more accurate than all but CCSD(T) for this subset, with an RMSD of 2.88 kcal/mol. Although AFQMC does not perform as well as

CCSD(T) for these data points, it is significantly more accurate than the other approaches considered here.

The good performance of CCSD(T) for these MR data points may be understood by the fact that many of these MR calculations are not necessarily strongly correlated ones. There are multiple ways to diagnose MR character, with different metrics providing distinct classifications. For example, if we use regularized orbital-optimized MP2 ( $\kappa$ -OOMP2)<sup>113</sup> and inspect the underlying spin-symmetry breaking of the solution, only 7 out of the 16 MR data points in the TAE140 set exhibit spin-symmetry breaking. Based on this, one would conclude that only 7 data points in TAE140 should be considered to carry MR character. We will discuss bond breaking examples in the later sections which will unambiguously fall into the strongly correlated category for stretched geometries.

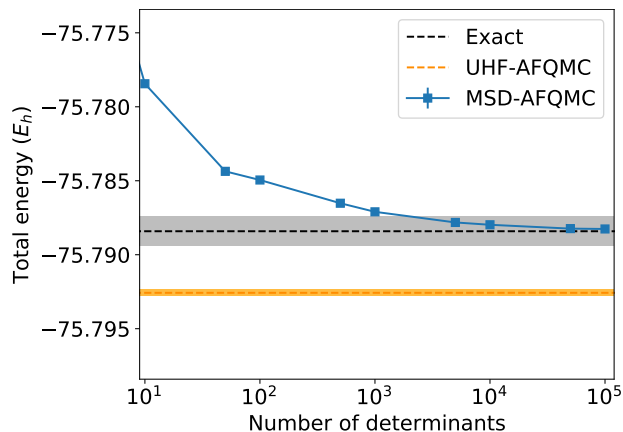


FIG. 4. Convergence of AFQMC energy ( $E_h$ ) with an MSD trial to the exact energy for  $C_2$  in aug-cc-pVTZ as a function of the number of determinants in the trial. Gray area indicates chemical accuracy (1 kcal/mol) from the exact answer. Dotted orange line and orange area denote UHF-AFQMC energy and its error bar. UHF-AFQMC and MSD-AFQMC mean AFQMC performed with UHF and MSD trials, respectively.

To emphasize the flexibility of AFQMC, we further study  $C_2$  in aug-cc-pVTZ which is one of the representative MR examples in the MR16 subset. We generate a large MSD trial using SHCI for an active space with 8-electron and 90-orbital. We then systematically converge AFQMC energies using that trial to the exact answer obtained by SHCI. As shown in Fig. 4, MSD-AFQMC quickly improves its accuracy as one adds more determinants to the trial and becomes chemically accurate with  $10^4$  determinants or so. Compared to more conventional quantum chemistry methods such as coupled-cluster theory, the generalization of AFQMC to MSD trials is rather straightforward and it can often be used to improve the results significantly beyond AFQMC with an SD trial. One can also try to find other MSD trials generated from a smaller active space to reduce the number of determinants needed to reach chemical accuracy.<sup>22</sup> We will see



the power of MSD-AFQMC more later in Section III C 2.

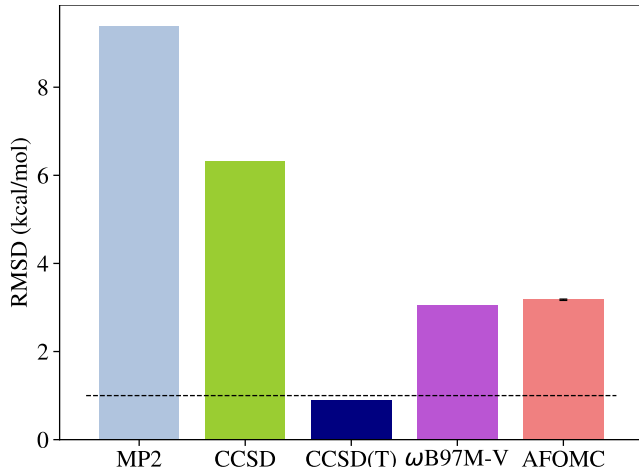


FIG. 5. Root-mean-square deviation (RMSD) for the entire W4-11 benchmark set. The black dotted lines indicate the “chemical accuracy” of 1 kcal/mol.

In summary, based on this thermochemistry benchmark study, we conclude that the performance of AFQMC with a simple SD trial is expected to provide accuracy that lies between CCSD and CCSD(T). It is also quite competitive with a state-of-the-art density functional,  $\omega$ B97M-V, which is *a priori* expected to be accurate for the class of systems studied here. These conclusions are summarized in Fig. 5. We thus recommend AFQMC with a simple SD trial for calculations where DFT is expected to struggle (either due to self-interaction error or due to strong correlation) and CCSD(T) is too expensive.

### B. Non-covalent interaction benchmark (A24)

A24 is a high-quality non-covalent interaction benchmark set composed of 24 small, non-covalently bound complexes.<sup>86</sup> All molecules in the set should be well described by RHF wave functions. For this set we employ RHF wave functions for both CC and AFQMC methods. We also used the counterpoise correction to eliminate the basis set superposition error. The energy scale in this set is quite small, with interaction energies ranging from 1.115 kcal/mol to -6.493 kcal/mol. In Fig. 6, we present the RMSD values of MP2, CCSD, CCSD(T),  $\omega$ B97M-V, and AFQMC for this set. MP2 has the largest RMSD (1.12 kcal/mol), while CCSD and CCSD(T) are nearly exact (RMSD = 0.05 kcal/mol).  $\omega$ B97M-V is also very accurate with an RMSD of 0.09 kcal/mol. AFQMC exhibits more sizable errors than do the CC methods, with an RMSD of 0.32(7) kcal/mol. This is about a factor of 4 larger error than  $\omega$ B97M-V, although still within chemical accuracy.

For relatively simple non-covalently bound systems, combinatorially optimized density functionals

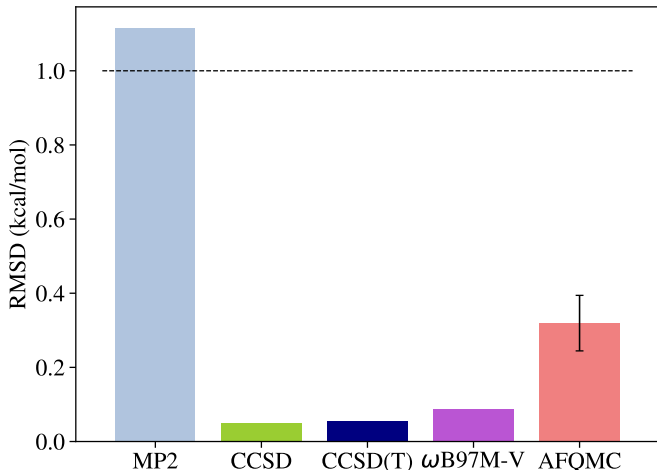


FIG. 6. Root-mean-square deviation (RMSD) for the A24 benchmark set. The black dotted lines indicate the “chemical accuracy” value of 1 kcal/mol.

like  $\omega$ B97M-V work well, approaching the accuracy of CCSD(T).<sup>131</sup> Therefore, we recommend the use of AFQMC for non-covalent interaction energies only if the system under study exhibits additional challenges for DFT, such as those arise in cases with open-shell electrons or self-interaction error. At the same time, the accuracy for AFQMC in such cases in comparison to CCSD(T) is still under-explored. Given the small energy scale and the small number of data points in A24, a more thorough investigation of non-covalent interactions with AFQMC is highly desirable. The recent report<sup>134</sup> by Tkatchenko and co-workers of significant deviations between diffusion Monte Carlo and CCSD(T) for large, non-covalently bound complexes thus provides a worthy target for a future investigation performed with AFQMC.

### C. Breaking chemical bonds

Bond breaking in simple molecular systems has been a test bed for the electronic structure treatment of strong correlation. This is because one can simply tune the strength of the electron correlation (i.e., the degree to which an SR wave function fails qualitatively) by changing the bond distance. This fact was recognized early in the development of AFQMC, as evidenced by the work of Zhang and co-workers.<sup>11,12,21–23</sup> In this section, we add more data to this body of work by considering  $H_4$  in STO-3G and cc-pVQZ bases and  $N_2$  (all-electron) in STO-3G and cc-pVTZ bases. STO-3G is a minimal basis set and is known to exaggerate strong correlation effects.<sup>135</sup> Therefore, bond breaking in the STO-3G basis set has been a particularly popular test for strong correlation methods.<sup>87–95</sup> Larger basis set examples will exhibit a mixture of strong and weak correlation effects, which is a common challenge encountered in realistic problems.

The geometry of  $H_4$  in  $\text{\AA}$  is

$$\begin{aligned} H1 &: (0, 0, 0), \\ H2 &: (0, 0, 1.23), \\ H3 &: (R_{H-H}, 0, 0), \\ H4 &: (R_{H-H}, 0, 1.23), \end{aligned}$$

where we vary the distance between two stretched  $H_2$  units, with each unit with a fixed bond distance of 1.23  $\text{\AA}$ . This value is selected because for  $R_{H-H} = 1.23 \text{\AA}$ , two RHF determinants become quasi-degenerate, maximizing the strong correlation aspect of this model. Thus RHF is qualitatively incorrect and UHF cannot fully remedy this problem. A natural active space for this problem is (4e,4o) (i.e., 4-electrons in 4-orbitals), and this is what we use to generate complete active space self-consistent field (CASSCF) states for our subsequent dynamic correlation treatment.

In the case of  $N_2$ , we vary the bond distance,  $R_{N-N}$ , between the two nitrogen atoms. As the bond is stretched,  $N_2$  exhibits strong correlation effects, and ultimately dissociates to two quartet nitrogen atoms. RHF cannot correctly dissociate  $N_2$  whereas UHF dissociates this molecule correctly. For large bond distances, UHF is therefore expected to be qualitatively correct, while RHF qualitatively fails. Nonetheless, for intermediate bond distances, UHF is incapable of describing spin-recoupling and will thus lead to quantitatively inaccurate results in this regime. For CASSCF, we use a minimal active space of (6e,6o) (i.e., 6-electrons in 6-orbitals).

To add dynamic correlation on top of the CASSCF calculation, we consider some of the more widely used multi-reference methods in addition to AFQMC. These methods are summarized in Table II along with their acronyms. For CASPT2 we did not use any shifts.<sup>149–152</sup> NEVPT2 is performed via the partially contracted algorithm,<sup>139</sup> whereas the rest of the deterministic MR methods employed fully internally contracted versions. These methods represent commonly used dynamic correlation approaches for MR systems.

### 1. Assessment of single-reference methods

We first discuss the performance of single-reference methods for  $H_4$ . In Fig. 7 (a), we present the error for each single-reference method for the STO-3G basis set. We examine both RHF and UHF states for CCSD(T) and AFQMC for use as reference or trial functions. These different calculations are referred to as RCCSD(T)/UCCSD(T) and RAFQMC/UAFQMC, respectively.

The sharp derivative discontinuity at  $R_{H-H} = 1.23 \text{\AA}$  in RCCSD(T) and RAFQMC is due to the two RHF solutions crossing at  $R_{H-H} = 1.23 \text{\AA}$ . As noted previously in literature,<sup>94</sup> RCCSD(T) becomes non-variational as the unit bond distance approaches  $R_{H-H} = 1.23 \text{\AA}$ . In the case of RAFQMC, the energy is always above

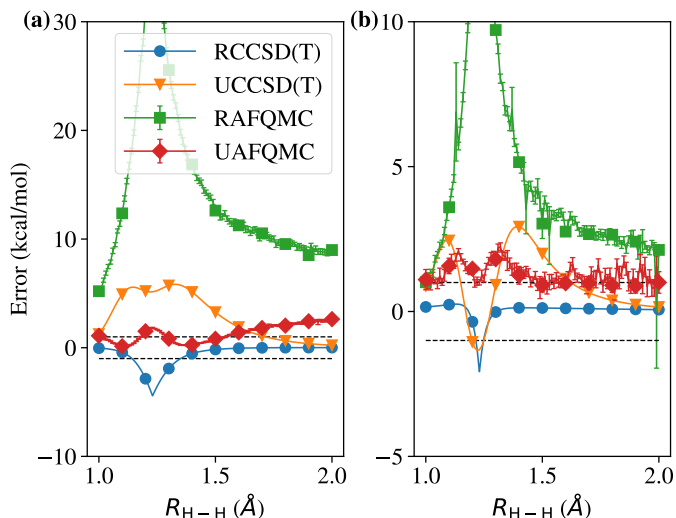


FIG. 7. Error in the potential energy curve of  $H_4$  as a function of  $R_{H-H}$  for methods based on HF states (a) using a STO-3G basis set and (b) using a cc-pVQZ basis set. Note that there are more data points than markers shown. See Fig. A2 for qualitative shapes of these potential energy curves in absolute energy scale.

the exact energy, but the magnitude of the error is about nine to ten times larger than that of RCCSD(T). UCCSD(T) produces variational energies at every distance considered here. UAFQMC performs far better than RAFQMC at every bond distance and also outperforms UCCSD(T) up to  $R_{H-H} = 1.64 \text{\AA}$ . This is highly encouraging because UAFQMC is very accurate near the distances where strong correlation is most pronounced. Nonetheless, UAFQMC does not dissociate this molecule into two independent  $H_2$  correctly. Both RCCSD(T) and UCCSD(T) correctly describe dissociation, but neither does RAFQMC nor UAFQMC. In Section III A 1, we discussed the exactness of CCSD(T) and the non-exactness of AFQMC for two-electron systems. The  $H_4 \rightarrow 2 H_2$  dissociation problem is thus another good illustration of this point.

We observe similar behavior of all four methods in the larger basis set, cc-pVQZ, as illustrated in Fig. 7 (b). Since strong correlation is less pronounced in a larger basis set, the magnitude of the error produced by all methods is significantly smaller compared to that exhibited in the STO-3G basis. Nonetheless, qualitative failures of RCCSD(T), such as non-variationality and a derivative discontinuity at the square geometry are still observed in this basis set. As is the case for the STO-3G basis, RAFQMC exhibits a significantly larger error than RCCSD(T) does in this basis set. Finally, we observe quite similar levels of quantitative accuracy when comparing UCCSD(T) to UAFQMC.

We continue the discussion of the performance of single-reference methods for  $N_2$  as shown in Fig. 8 for (a) STO-3G and (b) cc-pVTZ. Unlike  $H_4$ , we find that the errors exhibited by different methods are compa-

Acronym	Full Name	References
CASPT2	Complete Active Space Second-Order Perturbation Theory	136,137
NEVPT2	N-electron Valence Second-Order Perturbation Theory	138,139
MRMP2	Multireference Second-Order Møller-Plesset Perturbation Theory	140
MRACPF	Multireference Average Coupled Pair Functional	141
MRAQCC	Multireference Average Quadratic Coupled Cluster	142,143
MRCISD+Q	Multireference Configuration Interaction with Singles, Doubles, and Davidson correction	144,145
DSRG-MRPT2	Driven Similarity Renormalization Group Multireference Second-Order Perturbation Theory	146
DSRG-MRPT3	Driven Similarity Renormalization Group Multireference Third-Order Perturbation Theory	147
MR-LDSRG(2)	Multireference Linearized Driven Similarity Renormalization Group Truncated with Two-Body Operators	148

TABLE II. Summary of multi-reference methods considered for bond-breaking benchmark problems in this work.

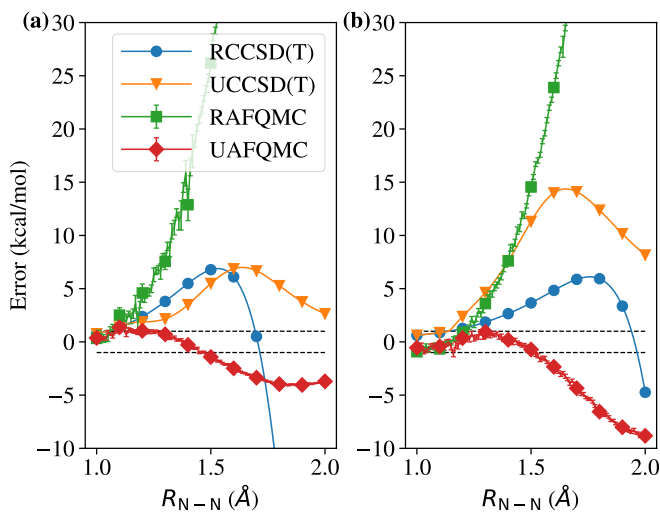


FIG. 8. Error in the potential energy curve of  $N_2$  as a function of  $R_{N-N}$  for methods based on HF states (a) using an STO-3G basis set and (b) using a cc-pVTZ basis set. Note that there are more data points than markers shown. See Fig. A2 for qualitative shapes of these potential energy curves in absolute energy scale.

table between these two bases sets. While there are multiple RHF solutions for  $N_2$ , we focused on the one that does not break spatial symmetry. RCCSD(T) exhibits incorrect turnover behavior and non-variationality at far distances, whereas UCCSD(T) has a large energy error in the spin-recoupling regime. UCCSD(T) ultimately dissociates correctly into two N atoms, but its error up to a bond distance  $R_{N-N} = 2 \text{ \AA}$  is quite sizable (7.5 kcal/mol for STO-3G and 15 kcal/mol for cc-pVTZ, respectively). RAFQMC again performs significantly worse than RCCSD(T). UAFQMC is quantitatively comparable to UCCSD(T) for both bases sets, but the sign of its error is opposite to that of UCCSD(T). We note that the fact that UAFQMC exhibits non-variationality is not unexpected, as AFQMC energies are not guaranteed to be variational.<sup>103</sup>

	$H_4$		$N_2$	
	STO-3G	cc-pVQZ	STO-3G	cc-pVTZ
RCCSD(T)	4.43	2.33	74.95	10.96
UCCSD(T)	5.61	4.28	6.23	13.80
RAFQMC	35.37(5)	18.65(36)	140.20(14)	87.72(23)
UAFQMC	2.51(8)	1.57(30)	5.89(16)	9.79(22)

TABLE III. Non-parallelity error (maximum error - minimum error) in kcal/mol for single-reference methods.

In summary, for bond breaking examples and other typical strongly correlated systems, it appears that RAFQMC exhibits significant errors, much larger than what is seen with RCCSD(T). However, UAFQMC is quantitatively better than UCCSD(T), although it is still far from chemical accuracy. This can be seen from the non-parallelity errors presented in Table III. Non-parallelity error is a commonly used metric for assessing the performance of different methods in the computation of the relative energetics on a potential energy surface. Therefore among single-reference methods, UAFQMC is a promising candidate for the treatment of relatively simple strongly correlated systems.

## 2. Assessment of multi-reference methods

We repeat the same analysis for MR methods where simple CASSCF states are employed either as a reference state or a trial wave function, and quantify the errors associated with the treatment of dynamic correlation. In Fig. 9, it is clear that the worst performer in terms of absolute energies in both  $H_2$  and  $N_2$  is NEVPT2. CASPT2 and MRMP2 perform much better than NEVPT2, by approximately 3 kcal/mol for  $H_2$  and by more than 10 kcal/mol for  $N_2$ . Nonetheless, in terms of non-parallelity error (NPE), see Table IV, NEVPT2 is comparable to CASPT2 and MRMP2 for  $H_4$  and is better than these two methods for  $N_2$  by more than 6 kcal/mol. CASPT2 and MRMP2 methods perform quite

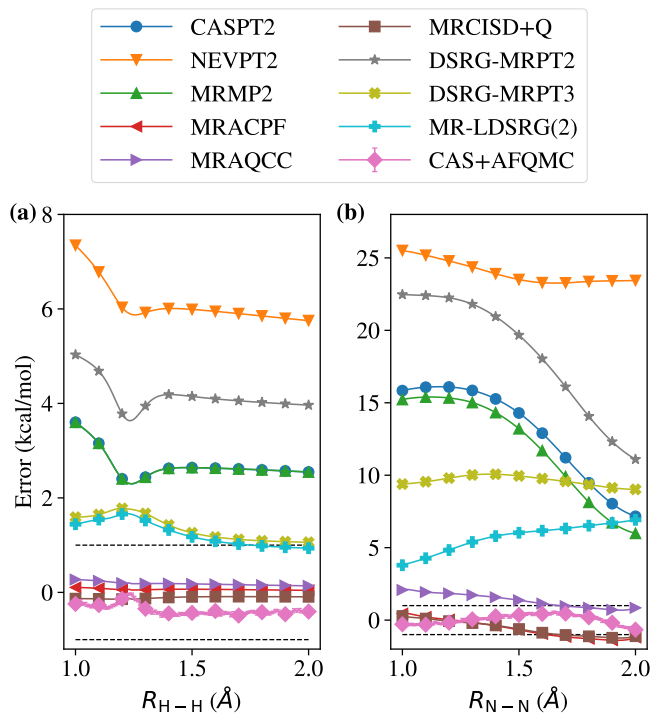


FIG. 9. Error in the potential energy curve of methods based on CASSCF states (a)  $H_4$  using a cc-pVQZ basis set and (b)  $N_2$  using a cc-pVTZ basis set. For  $H_4$ , MRMP2 and CASPT2 yield identical data. Note that there are more data points than markers shown. See Fig. A3 for qualitative shapes of these potential energy curves.

similarly (identically for  $H_4$ ), and their performance is far from the level of chemical accuracy. The performance of DSRG-MRPT2 falls between that of NEVPT2 and CASPT2/MRPT2. The poor performance of second-order perturbation theories is particularly worrying, as these methods are the most commonly employed MR methods due to their simplicity and their relatively inexpensive nature, namely a scaling of  $\mathcal{O}(N^5)$  outside the active space.

We have also investigated the performance of MR-CISD using different ways to correct for its size-inconsistency error (namely MRACPF, MRAQCC, MRCISD+Q). These methods are computationally more expensive than MRPT methods, with a scaling of  $\mathcal{O}(N^6)$  outside the active space. This scaling also applies to two DSRG methods, DSRG-MRPT3 and MR-LDSRG(2). MRACPF, MRAQCC, and MRCISD+Q are all nearly exact for  $H_4$ . MRAQCC becomes more inaccurate for  $N_2$ , exhibiting errors beyond chemical accuracy at small bond distances. Nonetheless, MRACPF and MRCISD+Q provide near-chemical accuracy for all bond distances for  $N_2$ . For both molecules, MR-LDSRG(2) is not as accurate as the MRCI methods for both absolute and relative energies. Nonetheless, for  $H_4$ , its NPE is only 0.73 kcal/mol. DSRG-MRPT3 performs very similarly to MR-LDSRG(2) for  $H_4$ , but it differs significantly from MR-LDSRG(2) for  $N_2$ . For  $N_2$ , DSRG-MRPT3 produces

	$H_4$	$N_2$
CASPT2	1.30	8.98
NEVPT2	1.59	2.29
MRMP2	1.30	9.43
DSRG-MRPT2	1.39	11.38
DSRG-MRPT3	0.72	1.16
MR-LDSRG(2)	0.73	3.16
MRACPF	0.06	2.08
MRAQCC	0.13	1.62
MRCISD+Q	0.05	1.67
CAS+AFQMC	0.48(2)	1.27(8)

TABLE IV. Non-parallelity error (maximum error - minimum error) in kcal/mol for multi-reference methods.

absolute energies that are quite far from chemical accuracy, but its NPE is quite small and comparable to that of MRCISD+Q and MRAQCC.

AFQMC with CASSCF trial wave functions works remarkably well for both  $H_2$  and  $N_2$  achieving chemical accuracy at all bond distances. This accuracy comes with a far lower scaling cost (see Table I) than both MRPT and MRCI-based methods, where we emphasize the steep scaling of these methods within the active space due to the requirement of higher-order density matrices. We also note that none of the other MR methods except NEVPT2 and the DSRG methods are size-consistent. Since CASSCF is size-consistent, AFQMC with CASSCF trial wave functions is also size-consistent in the limit of  $\Delta t \rightarrow 0$  (see Section IID).

Due to its computational efficiency and its accuracy in reproducing both absolute energies and NPE values (see Table IV), AFQMC would appear to be the method of choice when strong correlation can be handled by the CASSCF trial wave function and the remaining dynamic correlation needs to be corrected at scale. With the improved algorithm for using SCI trial wave functions,<sup>9</sup> AFQMC will likely become a commonly used MR dynamic correlation method in the future.

#### IV. OUTLOOK AND FUTURE OPPORTUNITIES

There are many future opportunities for developments and improvements of different aspects of ph-AFQMC. Due to its relatively new vintage and the comparatively limited use of the method in quantum chemistry, the development of ph-AFQMC when compared to, for example, CC methods has not yet reached full maturity. We note several promising opportunities for future development in this section.

1. *Trial wave functions:* As mentioned in Section IIB, the form of trial wave functions is currently limited to SD trials or relatively compact MSD trials. Using more accurate trial wave functions without greatly increasing the overall com-

putational cost is a forefront area for future ph-AFQMC development. Compared to CCSD(T), where going beyond the SD reference is formally challenging, the flexibility afforded by ph-AFQMC will lead to important developments along this line. Our experience suggests that the sensitivity to the trial wave function within ph-AFQMC is far greater than is the sensitivity of CC methods to the reference wave function. This both provides opportunities to greatly enhance accuracy but also challenges for rationally developing strategies for the use of trial functions.

2. *Alternative constraints:* Due to the lack of extensive benchmark studies, we do not know if the constraint provided by the cosine projection in Eq. (7) is optimal in terms of accuracy and statistical efficiency. As noted in Section II D, the currently used phaseless constraint introduces an  $\mathcal{O}(\Delta t)$  time step error, limiting the size of time steps and necessitating time step extrapolations beyond the Trotter error. Furthermore it may well be that different constraints provide different levels of accuracy even when used with the same trial wave function. Much more work in this direction is warranted.
3. *Observables other than ground state energies:* Some observable properties extracted from ph-AFQMC have been shown to be less reliable than is desirable.<sup>25,80</sup> The accuracy of properties computed via back propagation provides one concrete example. Furthermore, excited state energies also fall into this category where additional complications arise due to the nature of projector Monte Carlo. At this stage ph-AFQMC is an accurate method for the ground state energy in chemical systems, however ancillary algorithms that enable the computation of other properties with the accuracy consistent with that of the ground state energy within ph-AFQMC is an important goal for future research.
4. *Computational cost:* Local energy evaluation algorithms for ph-AFQMC with SD trial wave functions are relatively mature and provide multiple ways to reach cubic scaling per sample.<sup>5-8</sup> However, algorithms to accelerate walker propagation are scarce. In addition, local energy evaluation algorithms for ph-AFQMC with more complex MSD trial wave functions have been relatively less explored.<sup>8,9</sup> Thus, reducing the computational cost of all components in ph-AFQMC other than the local energy evaluation forms another direction worthy of future effort.

## V. CONCLUSIONS

The purpose of this work has been two-fold: First, we have presented a self-contained overview of the formalism behind the ph-AFQMC approach from a quantum chemistry perspective, and have delineated the considerations needed to understand the computational implementation and cost of the approach. Second, we have assessed the performance of ph-AFQMC for a well-known main group chemistry benchmark set (W4-11) and a non-covalent interaction benchmark set (A24), leading to a total of 1004 relative energies. In addition, we have studied the potential energy curves of commonly studied model problems, namely  $H_4$  and  $N_2$ , documenting the performance of ph-AFQMC with different trial wave functions against other standard wave function-based quantum chemistry methods. This constitutes the largest quantum chemical benchmark study to date using ph-AFQMC. While the knowledge gained from our work is far from complete, we will conclude our work with some cautious recommendations for the use of ph-AFQMC in a broad chemical context.

*Single Slater determinant trial wave functions:* ph-AFQMC employed with a with single determinant trial is an accurate method that can be a method of choice if CCSD(T) is too expensive and if the target system does not exhibit open-shell electrons with sizable antiferromagnetic coupling. While studies on chemical systems using DMC and GFMC have been limited, AFQMC was shown to be more accurate than these for the same single determinant trial for several specific systems.<sup>15,153</sup> Such trials will generally take the form of HF wave functions, or DFT<sup>10,66</sup> or regularized OOMP2<sup>16,113</sup> wave functions when HF exhibits unphysical properties such as over-localization. The performance of ph-AFQMC for non-covalent interaction energies is still unclear due to the limited number of data points we have considered. We hope that the community will take up the task of a more detailed investigation in the near future.

*Multi-Slater determinant trial wave functions:* For systems exhibiting open-shell electrons with antiferromagnetic coupling either due to bond breaking or arising from localized d- or f-electrons, ph-AFQMC must be used with more elaborate multi-Slater trial wave functions such as CASSCF or SCI wave functions. Using spin-unrestricted single determinant trials can be an option if there are only two electrons contributing to the strong correlation behavior.<sup>16,154</sup> However, the phaseless error needs to be carefully quantified by more sophisticated trial wave functions in realistic strongly correlated if possible. We stress that ph-AFQMC was found to be far more accurate than other MRPT methods, such as CASPT2, NEVPT2, and MRMP2. Given its high efficiency compared to MRCI methods, we anticipate ph-AFQMC to become a clear method of choice for including dynamic correlation in active-space calculations. With improved algorithms<sup>9</sup> and implementations leveraging graphical processing units (GPUs),<sup>28,76</sup> we believe

that ph-AFQMC with  $\sim 10^5$  to  $10^6$  determinants will become routine calculations. Nonetheless, enabling the efficient use of sophisticated trial wave functions is one of the most pressing topics for near-term development of ph-AFQMC.<sup>37,51,118,119</sup>

We hope that the numerical data presented in this work, as well as the existence of currently available open-source packages<sup>81–83</sup> will encourage many more developers and users to explore uncharted territory and contribute to method development within the ph-AFQMC framework. While the data provided here constitutes the most extensive data set for ph-AFQMC to date, it is important to continue producing data and comparisons for a wide class of systems. Furthermore, compared to other deterministic quantum chemistry methods, ph-AFQMC is not yet at the stage of development where it can be considered a “black-box” approach. In addition, its final energy is also statistical in nature, introducing additional barrier for users to use the method. It is, therefore, important to have and further develop open-source frameworks<sup>82,83</sup> and to provide straightforward user interfaces. Such efforts will enable the expansion of our understanding of the relative benefits and weaknesses of ph-AFQMC, and we hope this goal is taken up by the electronic structure community with enthusiasm in the coming years.

## VI. ACKNOWLEDGMENT

We thank Luke Bertels, Garnet Chan, Francesco Evangelista, Fionn Malone, Adam Rettig, Sandeep Sharma, and Shiwei Zhang for helpful discussions. DRR would like to thank Richard Friesner and Shiwei Zhang for collaboration on AFQMC-related topics over the last several years. We thank Richard Friesner for the suggestion to carefully consider basis set extrapolations in this work. We thank Google for their gift that was used to support JL and HQP in developing a code used in this work. We also thank Francesco Evangelista for providing the bond dissociation data of  $H_4$  and  $N_2$  for the DSRG methods. We acknowledge computing resources from Columbia University’s Shared Research Computing Facility project, which is supported by NIH Research Facility Improvement Grant 1G20RR030893-01, and associated funds from the New York State Empire State Development, Division of Science Technology and Innovation (NYSTAR) Contract C090171, both awarded April 15, 2010.

## VII. APPENDIX

### A1. Further details on ground-state calculations

Discretizing imaginary time, one may write the imaginary time propagation in Eq. (1) as a product of infinitesimal

propagators

$$e^{-\tau\hat{H}} = \left(e^{-\Delta\tau\hat{H}}\right)^N, \quad (\text{A1})$$

where  $N$  is the total number of imaginary time steps and the small imaginary time step is defined as  $\Delta\tau = \tau/N$ .

The efficiency of AFQMC relies on the representation of the short-time propagator. One first recasts  $\hat{H}$  in Eq. (2) into

$$\hat{H} = \hat{H}_1 - \frac{1}{2} \sum_{\gamma=1}^{N_\gamma} \hat{v}_\gamma^2, \quad (\text{A2})$$

where  $\hat{H}_1$  is the one-body part of the Hamiltonian,

$$\hat{H}_1 = \sum_{pq} (h_{pq} - \frac{1}{2} \sum_r (pr|rq)) a_p^\dagger a_q, \quad (\text{A3})$$

and the two-body part is written as the sum of  $N_\gamma$  squared operators, for example, by using the modified Cholesky decomposition<sup>155,156</sup> or density fitting,<sup>157,158</sup>

$$\hat{v}_\gamma = \sum_{pr} L_{pr}^\gamma a_p^\dagger a_r, \quad (\text{A4})$$

with

$$(pr|qs) = \sum_{\gamma=1}^{N_\gamma} L_{pr}^\gamma L_{qs}^\gamma. \quad (\text{A5})$$

In practice, we modify this Hamiltonian further by performing a mean-field subtraction<sup>18</sup> or using a shifted contour<sup>36</sup>. This amounts to writing

$$\hat{v}'_\gamma = \hat{v}_\gamma - \langle \Psi_T | \hat{v}_\gamma | \Psi_T \rangle. \quad (\text{A6})$$

To realize Eq. (1) in a computationally efficient manner, we write the global wave function as a weighted summation over a statistical sample of wave functions,  $\{|\psi_i\rangle\}$ , commonly referred to as “walkers”:

$$|\Psi(\tau)\rangle = \sum_{i=1}^{N_{\text{walkers}}} w_i(\tau) |\psi_i(\tau)\rangle, \quad (\text{A7})$$

where  $w_i(\tau)$  is the weight of the  $i$ -th walker at imaginary time  $\tau$ . We also express  $\hat{B}(\mathbf{x})$  in Eq. (3) as

$$\hat{B}(\mathbf{x}) = \exp\left(-\Delta\tau\hat{H}_1\right) \exp\left(\sqrt{\Delta\tau} \sum_{\gamma=1}^{N_\gamma} x_\gamma \hat{v}'_\gamma\right). \quad (\text{A8})$$

An instance of the short-time propagator in Eq. (A8) is then applied to a set of random walkers  $\{|\psi_i\rangle\}$  to obtain the ground state  $|\Psi_0\rangle$  from the initial state. Namely, each walker is assigned to a vector of Gaussian random variables  $\mathbf{x}_i(\tau)$  at imaginary time  $\tau$  and one applies Eq. (A8) to advance the wave function to the next time step

$$|\psi_i(\tau + \Delta\tau)\rangle = \hat{B}(\mathbf{x}_i(\tau)) |\psi_i(\tau)\rangle. \quad (\text{A9})$$

This procedure effectively computes the high-dimensional integral in Eq. (3) by means of Monte Carlo sampling. Single Slater determinants are the most common form of walker wave functions, and the Thouless theorem ensures that the walkers will stay in the single Slater determinant manifold upon the action of the propagator.<sup>159,160</sup>

Global estimates for operators that commute with  $\hat{H}$  are evaluated by the following mixed estimator

$$\langle O(\tau) \rangle_{\text{mixed}} = \frac{\langle \Psi_T | \hat{O} | \Psi(\tau) \rangle}{\langle \Psi_T | \Psi(\tau) \rangle}, \quad (\text{A10})$$

where  $|\Psi_T\rangle$  is a wave function that allows for a straightforward evaluation of the above expression. If  $\hat{O} = \hat{H}$ , this provides an unbiased way to estimate the total energy. The algorithm discussed so far is defined as the free-projection AFQMC (fp-AFQMC) which is exact in principle, however, suffers from the phase (sign) problem.<sup>66</sup> Due to this problem, the mixed estimate in Eq. (A10) will generically have a variance that scales exponentially with system size.<sup>38</sup>

One way to control the severe statistical fluctuation arising from the phase problem is to use the phaseless approximation,<sup>66</sup> resulting in the phaseless AFQMC method (ph-AFQMC). ph-AFQMC utilizes importance sampling based on a trial wave function  $|\Psi_T\rangle$  throughout the random walk process and thereby works with the statistical representation of global wave functions as in Eq. (4). Given this importance sampling, the walker weight update rule follows

$$w_i(\tau + \Delta\tau) = w_i(\tau) \times I(\mathbf{x}_i(\tau), \bar{\mathbf{x}}_i(\tau), |\psi_i(\tau)\rangle), \quad (\text{A11})$$

where the importance function  $I$  which is proportional to the overlap ratio in Eq. (6) is given by

$$I(\mathbf{x}_i(\tau), \bar{\mathbf{x}}_i(\tau), |\psi_i(\tau)\rangle) = S(\mathbf{x}_i(\tau) - \bar{\mathbf{x}}_i(\tau), |\psi_i(\tau)\rangle) \times e^{\mathbf{x}_i(\tau)\bar{\mathbf{x}}_i(\tau) - \bar{\mathbf{x}}_i(\tau)\bar{\mathbf{x}}_i(\tau)/2}. \quad (\text{A12})$$

$\bar{\mathbf{x}}_i(\tau)$  is usually referred to as the optimal force bias<sup>97</sup> which provides a shift to the underlying normal distribution. The optimal force bias is computed as

$$\begin{aligned} \bar{x}_{\gamma,i}(\tau) &= -\sqrt{\Delta\tau} \frac{\langle \Psi_T | \hat{v}'_{\gamma} | \psi_i(\tau) \rangle}{\langle \Psi_T | \psi_i(\tau) \rangle} \\ &= -\sqrt{\Delta\tau} \sum_{pq} L_{pq}^{\gamma} G_{qp,i}(\tau), \end{aligned} \quad (\text{A13})$$

where the one-body Green's function  $G_{qp,i}(\tau)$  is given by

$$G_{qp,i}(\tau) = \frac{\langle \Psi_T | a_p^{\dagger} a_q | \psi_i(\tau) \rangle}{\langle \Psi_T | \psi_i(\tau) \rangle}. \quad (\text{A14})$$

Beyond Eq. (A11), ph-AFQMC imposes a constraint to ensure the positivity of the weights throughout the imaginary time propagation. Such a constraint is achieved by a modified importance function,  $I_{\text{ph}}$ ,

$$I_{\text{ph}}(\mathbf{x}_i(\tau), \bar{\mathbf{x}}_i(\tau), |\psi_i(\tau)\rangle) = \|I(\mathbf{x}_i(\tau), \bar{\mathbf{x}}_i(\tau), |\psi_i(\tau)\rangle)\| \times \max(0, \cos \theta_i(\tau)), \quad (\text{A15})$$

where the phase  $\theta_i(\tau)$  is given in Eq. (8). This modified importance function is used in ph-AFQMC to update the weights.

## A2. Numerical investigation of size-consistency

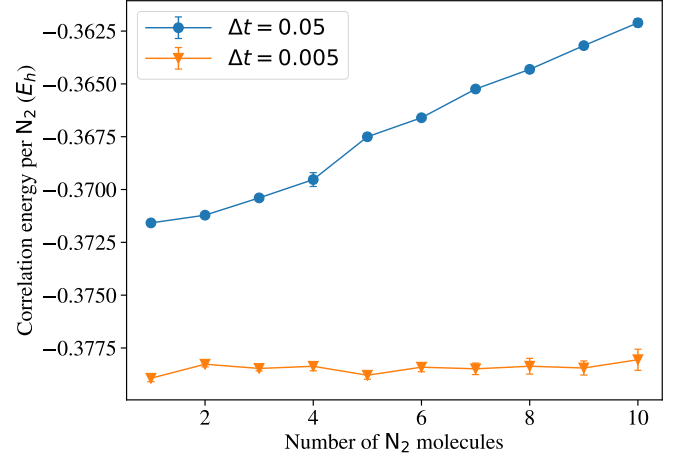


FIG. A1. Correlation energy per N<sub>2</sub> molecule as a function of the number of N<sub>2</sub> molecules that are infinitely far apart from each other for  $\Delta t = 0.05$  a.u. (round, blue) and  $\Delta t = 0.005$  a.u. (triangle, orange).

We verify the size-inconsistency error of ph-AFQMC with a finite time step via numerical results on N<sub>2</sub> at a bond distance of 1.3 Å and with an RHF trial wave function in the cc-pVDZ basis.<sup>161</sup> We add N<sub>2</sub> molecules at infinite separation. One should expect the correlation energy per molecule to be constant if the method was size-consistent. We used 640 walkers and checked that this result is not due to the population control bias. As shown in Fig. A1, for a relatively large time step ( $\Delta t = 0.05$  a.u.), the correlation energy per molecule decreases as we add more N<sub>2</sub> molecules to the system. Going from one N<sub>2</sub> molecule to 10 N<sub>2</sub> molecules, we observe the change in the correlation energy per molecule by 10 mE<sub>h</sub> for  $\Delta = 0.05$  a.u. This confirms that ph-AFQMC is in general not size-consistent as illustrated by Eq. (16). We do not see such a large error in the case of a smaller time step ( $\Delta t = 0.005$  a.u.). For larger systems, we anticipate that  $\Delta t = 0.005$  a.u. would not be small enough to completely eliminate this error, and thus one must be cautious with respect to time step and the possibility of size-inconsistency. We also emphasize that when quantifying the size-inconsistency error in this numerical experiment, the typical time step error caused by the Trotter error in Eq. (3) is the same for each fragment. Therefore, our result is not due to the time step error during the Trotterization, and is solely caused by the lack of size-consistency in ph-AFQMC for finite  $\Delta t$ .

### A3. Additional computational details concerning benchmark data

We used 640 walkers in all systems considered here and the corresponding population control bias was found to be negligible with the pair-branch algorithm.<sup>162</sup> A time step of 0.005 au was used and the time step error (for both Trotterization and size-consistency) was found to be also negligible at the energy scale we focus on in this work. The frozen core approximation was used throughout unless specified otherwise.

For the W4-11 set,<sup>85</sup> we used the aug-cc-pV5Z basis set<sup>161</sup> to converge the Hartree-Fock (HF) energies to the basis set limit and used aug-cc-pVTZ<sup>161</sup> and aug-cc-pVQZ<sup>161</sup> to extrapolate the correlation energies to the basis set limit following Helgaker’s two-point extrapolation.<sup>163</sup> We also use Karton and Martin’s inner-shell correlation energy contribution to correct for the missing core correlation energy due to the frozen core approximation.<sup>85</sup> Furthermore, to estimate the residual basis set error due to the differences in our scheme and Karton and Martin’s scheme, we also compared our CCSD(T) relative energies and their reported CCSD(T) relative energies. The root-mean-square-deviation of the difference was 0.66 kcal/mol which is small enough for the purpose of this paper. We note that Karton and Martin used the composite W4 scheme to estimate reference energies which involved up to CCSDTQ5 or CCSDTQ6. For the A24 set,<sup>86</sup> we used aug-cc-pVTZ<sup>161</sup> with counterpoise corrections, although the reference data (i.e., CCSD with triples and perturbative quadruples) were obtained in the basis set limit. For H<sub>4</sub> and N<sub>2</sub> dissociation data, we used cc-pVQZ and cc-pVTZ, respectively, bases<sup>161</sup> without the frozen core approximation.

Molecular integrals for ph-AFQMC were generated by PySCF,<sup>164</sup> all deterministic single-reference quantum chemistry calculations were performed with Q-Chem,<sup>165</sup> and AFQMC calculations were performed with the ipie<sup>82,83</sup> and QMCPACK.<sup>81</sup> Cholesky factorization and integral transformations necessary for AFQMC calculations were performed by a script in ipie<sup>82,83</sup> with a Cholesky threshold of 10<sup>-5</sup>. Semistochastic heat-bath configuration interaction (SHCI) calculations were performed with Dice.<sup>166</sup> Multi-reference dynamic correlation methods other than driven similarity renormalization group (DSRG) methods were run on Orca.<sup>167</sup> DSRG methods were run through Psi4 with the flow parameter  $\sigma = 0.5$  a.u..<sup>168</sup> DSRG-MRPT2 and DSRG-MRPT3 energies were obtained via the partial relaxation scheme.<sup>147</sup>

MR-LDSRG(2) energies were obtained by relaxing the reference state twice.<sup>148</sup>

We used SHCI to generate near-exact benchmark energies for bond dissociation examples. SHCI energies are converged more accurately than 0.1 mE<sub>h</sub>, except for N<sub>2</sub> in the cc-pVTZ basis. For N<sub>2</sub> in the cc-pVTZ basis, we estimate the remaining bias in our SHCI energies to be less than 1 kcal/mol. The second-order perturbation theory (PT2) contribution was found to be at most 10 mE<sub>h</sub> for this system and we did not perform any extrapolation to reduce the potential bias further. The SHCI energies used in this work are within 1 mE<sub>h</sub> of the SHCI energies from our recent investigation of N<sub>2</sub> in the cc-pVTZ basis at a limited set of bond distances<sup>119</sup> where the PT2 contribution in SHCI was converged to better than 2 mE<sub>h</sub>. We believe that the residual bias in SHCI energies is small enough that our conclusions are not affected by this bias.  $\omega$ B97M-V results are taken from ref. 2

All relevant raw energies are available in the Zenodo repository.<sup>130</sup>

### A4. Potential energy curves of H<sub>4</sub> and N<sub>2</sub> in STO-3G

We present the potential energy curve of H<sub>4</sub> and N<sub>2</sub> using an STO-3G basis set with single-reference methods in Fig. A2 and multi-reference methods in Fig. A3. This is to give the reader a visual sense for the potential energy curves for each of these problems.

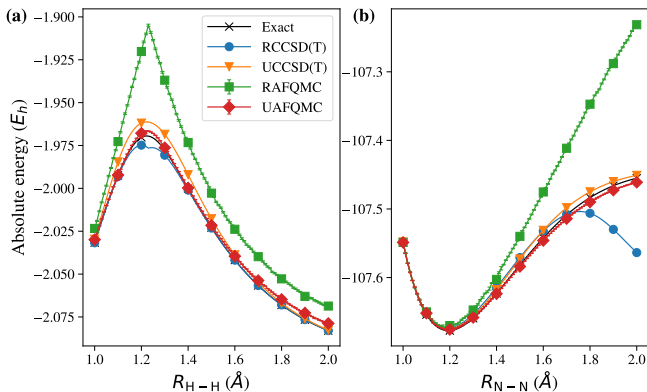


FIG. A2. The potential energy curve of (a) H<sub>4</sub> and (b) N<sub>2</sub> as a function of the bond distance using an STO-3G basis set. Note that there are more data points than markers shown.

\* [linusjoonho@gmail.com](mailto:linusjoonho@gmail.com)

<sup>1</sup> Trygve Helgaker, Poul Jorgensen, and Jeppe Olsen, *Molecular electronic-structure theory* (John Wiley & Sons, 2014).

<sup>2</sup> Narbe Mardirossian and Martin Head-Gordon, “Thirty years of density functional theory in computational chem-

istry: An overview and extensive assessment of 200 density functionals,” *Mol. Phys.* **115**, 2315–2372 (2017).

<sup>3</sup> Aron J. Cohen, Paula Mori-Sánchez, and Weitao Yang, “Challenges for Density Functional Theory,” *Chem. Rev.* **112**, 289–320 (2012).



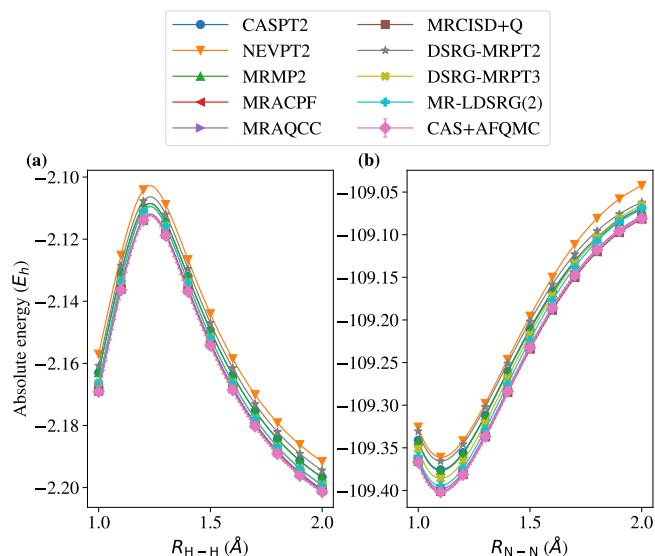


FIG. A3. The potential energy curve of (a)  $H_4$  in cc-pVQZ and (b)  $N_2$  in cc-pVTZ as a function of the bond distance using multi-reference methods. Note that there are more data points than markers shown.

- 4 Rodney J. Bartlett and Monika Musiał, “Coupled-cluster theory in quantum chemistry,” *Rev. Mod. Phys.* **79**, 291 (2007).
- 5 Fionn D. Malone, Shuai Zhang, and Miguel A. Morales, “Overcoming the Memory Bottleneck in Auxiliary Field Quantum Monte Carlo Simulations with Interpolative Separable Density Fitting,” *J. Chem. Theory Comput.* **15**, 256–264 (2019).
- 6 Mario Motta, James Shee, Shiwei Zhang, and Garnet Kin-Lic Chan, “Efficient Ab Initio Auxiliary-Field Quantum Monte Carlo Calculations in Gaussian Bases via Low-Rank Tensor Decomposition,” *J. Chem. Theory Comput.* **15**, 3510–3521 (2019).
- 7 Joonho Lee and David R. Reichman, “Stochastic resolution-of-the-identity auxiliary-field quantum Monte Carlo: Scaling reduction without overhead,” *J. Chem. Phys.* **153**, 044131 (2020).
- 8 John L. Weber, Hung Vuong, Pierre A. Devlaminck, James Shee, Joonho Lee, David R. Reichman, and Richard A. Friesner, “A Localized-Orbital Energy Evaluation for Auxiliary-Field Quantum Monte Carlo,” *J. Chem. Theory Comput.* **18**, 3447–3459 (2022).
- 9 Ankit Mahajan, Joonho Lee, and Sandeep Sharma, “Selected configuration interaction wave functions in phaseless auxiliary field quantum Monte Carlo,” *J. Chem. Phys.* **156**, 174111 (2022).
- 10 WA Al-Saidi, Henry Krakauer, and Shiwei Zhang, “Auxiliary-field quantum monte carlo study of tio and mno molecules,” *Phys. Rev. B* **73**, 075103 (2006).
- 11 Wirawan Purwanto, Shiwei Zhang, and Henry Krakauer, “An auxiliary-field quantum Monte Carlo study of the chromium dimer,” *J. Chem. Phys.* **142**, 064302 (2015).
- 12 Wirawan Purwanto, Shiwei Zhang, and Henry Krakauer, “Auxiliary-field quantum Monte Carlo calculations of the molybdenum dimer,” *J. Chem. Phys.* **144**, 244306 (2016).
- 13 James Shee, Benjamin Rudsteyn, Evan J. Arthur, Shiwei Zhang, David R. Reichman, and Richard A. Friesner, “On Achieving High Accuracy in Quantum Chemical Calculations of 3d Transition Metal-Containing Systems: A Comparison of Auxiliary-Field Quantum Monte Carlo with Coupled Cluster, Density Functional Theory, and Experiment for Diatomic Molecules,” *J. Chem. Theory Comput.* **15**, 2346–2358 (2019).
- 14 Benjamin Rudsteyn, Dilek Coskun, John L. Weber, Evan J. Arthur, Shiwei Zhang, David R. Reichman, Richard A. Friesner, and James Shee, “Predicting Ligand-Dissociation Energies of 3d Coordination Complexes with Auxiliary-Field Quantum Monte Carlo,” *J. Chem. Theory Comput.* **16**, 3041–3054 (2020).
- 15 Kiel T Williams, Yuan Yao, Jia Li, Li Chen, Hao Shi, Mario Motta, Chunyao Niu, Ushnish Ray, Sheng Guo, Robert J Anderson, *et al.*, “Direct comparison of many-body methods for realistic electronic hamiltonians,” *Phys. Rev. X* **10**, 011041 (2020).
- 16 Joonho Lee, Fionn D. Malone, and Miguel A. Morales, “Utilizing Essential Symmetry Breaking in Auxiliary-Field Quantum Monte Carlo: Application to the Spin Gaps of the  $C_{36}$  Fullerene and an Iron Porphyrin Model Complex,” *J. Chem. Theory Comput.* **16**, 3019–3027 (2020).
- 17 Benjamin Rudsteyn, John L. Weber, Dilek Coskun, Pierre A. Devlaminck, Shiwei Zhang, David R. Reichman, James Shee, and Richard A. Friesner, “Calculation of Metallocene Ionization Potentials via Auxiliary Field Quantum Monte Carlo: Toward Benchmark Quantum Chemistry for Transition Metals,” *J. Chem. Theory Comput.* **18**, 2845–2862 (2022).
- 18 W. A. Al-Saidi, Shiwei Zhang, and Henry Krakauer, “Auxiliary-field quantum Monte Carlo calculations of molecular systems with a Gaussian basis,” *J. Chem. Phys.* **124**, 224101 (2006).
- 19 Malliga Suewattana, Wirawan Purwanto, Shiwei Zhang, Henry Krakauer, and Eric J Walter, “Phaseless auxiliary-field quantum monte carlo calculations with plane waves and pseudopotentials: Applications to atoms and molecules,” *Phys. Rev. B* **75**, 245123 (2007).
- 20 W. A. Al-Saidi, Henry Krakauer, and Shiwei Zhang, “A study of H+H2 and several H-bonded molecules by phaseless auxiliary-field quantum Monte Carlo with plane wave and Gaussian basis sets,” *J. Chem. Phys.* **126**, 194105 (2007).
- 21 W. A. Al-Saidi, Shiwei Zhang, and Henry Krakauer, “Bond breaking with auxiliary-field quantum Monte Carlo,” *J. Chem. Phys.* **127**, 144101 (2007).
- 22 Wirawan Purwanto, Shiwei Zhang, and Henry Krakauer, “Excited state calculations using phaseless auxiliary-field quantum Monte Carlo: Potential energy curves of low-lying  $C_2$  singlet states,” *J. Chem. Phys.* **130**, 094107 (2009).
- 23 Wirawan Purwanto, W. A. Al-Saidi, Henry Krakauer, and Shiwei Zhang, “Eliminating spin contamination in auxiliary-field quantum Monte Carlo: Realistic potential energy curve of  $F_2$ ,” *J. Chem. Phys.* **128**, 114309 (2008).
- 24 Wirawan Purwanto, Henry Krakauer, Yudistira Virgus, and Shiwei Zhang, “Assessing weak hydrogen binding on  $Ca^+$  centers: An accurate many-body study with large basis sets,” *J. Chem. Phys.* **135**, 164105 (2011).
- 25 Mario Motta and Shiwei Zhang, “Computation of Ground-State Properties in Molecular Systems: Back-Propagation with Auxiliary-Field Quantum Monte Carlo,” *J. Chem. Theory Comput.* **13**, 5367–5378 (2017).

- <sup>26</sup> James Shee, Shiwei Zhang, David R. Reichman, and Richard A. Friesner, “Chemical Transformations Approaching Chemical Accuracy via Correlated Sampling in Auxiliary-Field Quantum Monte Carlo,” *J. Chem. Theory Comput.* **13**, 2667–2680 (2017).
- <sup>27</sup> Mario Motta and Shiwei Zhang, “Communication: Calculation of interatomic forces and optimization of molecular geometry with auxiliary-field quantum Monte Carlo,” *J. Chem. Phys.* **148**, 181101 (2018).
- <sup>28</sup> James Shee, Evan J. Arthur, Shiwei Zhang, David R. Reichman, and Richard A. Friesner, “Phaseless Auxiliary-Field Quantum Monte Carlo on Graphical Processing Units,” *J. Chem. Theory Comput.* **14**, 4109–4121 (2018).
- <sup>29</sup> James Shee, Evan J. Arthur, Shiwei Zhang, David R. Reichman, and Richard A. Friesner, “Singlet–Triplet Energy Gaps of Organic Biradicals and Polyacenes with Auxiliary-Field Quantum Monte Carlo,” *J. Chem. Theory Comput.* **15**, 4924–4932 (2019).
- <sup>30</sup> Edgar Josué Landinez Borda, John Gomez, and Miguel A. Morales, “Non-orthogonal multi-Slater determinant expansions in auxiliary field quantum Monte Carlo,” *J. Chem. Phys.* **150**, 074105 (2019).
- <sup>31</sup> Joonho Lee, Fionn D. Malone, and David R. Reichman, “The performance of phaseless auxiliary-field quantum Monte Carlo on the ground state electronic energy of benzene,” *J. Chem. Phys.* **153**, 126101 (2020).
- <sup>32</sup> R. Blankenbecler, D. J. Scalapino, and R. L. Sugar, “Monte Carlo calculations of coupled boson-fermion systems. I,” *Phys. Rev. D* **24**, 2278–2286 (1981).
- <sup>33</sup> J. E. Hirsch, “Two-dimensional Hubbard model: Numerical simulation study,” *Phys. Rev. B* **31**, 4403–4419 (1985).
- <sup>34</sup> Pier Luigi Silvestrelli, Stefano Baroni, and Roberto Car, “Auxiliary-field quantum Monte Carlo calculations for systems with long-range repulsive interactions,” *Phys. Rev. Lett.* **71**, 1148–1151 (1993).
- <sup>35</sup> D. M. Charutz and Daniel Neuhauser, “Electronic structure via the auxiliary-field Monte Carlo algorithm,” *J. Chem. Phys.* **102**, 4495–4504 (1995).
- <sup>36</sup> Naomi Rom, Eyal Fattal, Ashish K. Gupta, Emily A. Carter, and Daniel Neuhauser, “Shifted-contour auxiliary-field Monte Carlo for molecular electronic structure,” *J. Chem. Phys.* **109**, 8241–8248 (1998).
- <sup>37</sup> Ankit Mahajan and Sandeep Sharma, “Taming the Sign Problem in Auxiliary-Field Quantum Monte Carlo Using Accurate Wave Functions,” *J. Chem. Theory Comput.* **17**, 4786–4798 (2021).
- <sup>38</sup> Matthias Troyer and Uwe-Jens Wiese, “Computational Complexity and Fundamental Limitations to Fermionic Quantum Monte Carlo Simulations,” *Phys. Rev. Lett.* **94**, 170201 (2005).
- <sup>39</sup> S. B. Fahy and D. R. Hamann, “Positive-projection Monte Carlo simulation: A new variational approach to strongly interacting fermion systems,” *Phys. Rev. Lett.* **65**, 3437–3440 (1990).
- <sup>40</sup> Jules W. Moskowitz, K. E. Schmidt, Michael A. Lee, and M. H. Kalos, “A new look at correlation energy in atomic and molecular systems. II. The application of the Green’s function Monte Carlo method to LiH,” *J. Chem. Phys.* **77**, 349–355 (1982).
- <sup>41</sup> H. J. M. van Bommel, D. F. B. Ten Haaf, W. van Saarloos, J. M. J. van Leeuwen, and G. An, “Fixed-Node Quantum Monte Carlo Method for Lattice Fermions,” *Phys. Rev. Lett.* **72**, 2442–2445 (1994).
- <sup>42</sup> D. M. Ceperley and B. J. Alder, “Ground State of the Electron Gas by a Stochastic Method,” *Phys. Rev. Lett.* **45**, 566–569 (1980).
- <sup>43</sup> Shiwei Zhang, J. Carlson, and J. E. Gubernatis, “Constrained Path Quantum Monte Carlo Method for Fermion Ground States,” *Phys. Rev. Lett.* **74**, 3652–3655 (1995).
- <sup>44</sup> Shiwei Zhang, J. Carlson, and J. E. Gubernatis, “Pairing Correlations in the Two-Dimensional Hubbard Model,” *Phys. Rev. Lett.* **78**, 4486–4489 (1997).
- <sup>45</sup> M. Guerrero, J. E. Gubernatis, and Shiwei Zhang, “Quantum Monte Carlo study of hole binding and pairing correlations in the three-band Hubbard model,” *Phys. Rev. B* **57**, 11980–11988 (1998).
- <sup>46</sup> M. Enjalran, F. Hébert, G. G. Batrouni, R. T. Scalettar, and Shiwei Zhang, “Constrained-path quantum Monte Carlo simulations of the zero-temperature disordered two-dimensional Hubbard model,” *Phys. Rev. B* **64**, 184402 (2001).
- <sup>47</sup> Chia-Chen Chang and Shiwei Zhang, “Spatially inhomogeneous phase in the two-dimensional repulsive Hubbard model,” *Phys. Rev. B* **78**, 165101 (2008).
- <sup>48</sup> Hao Shi and Shiwei Zhang, “Symmetry in auxiliary-field quantum Monte Carlo calculations,” *Phys. Rev. B* **88**, 125132 (2013).
- <sup>49</sup> Simons Collaboration on the Many-Electron Problem, J. P. F. LeBlanc, Andrey E. Antipov, Federico Becca, Ireneusz W. Bulik, Garnet Kin-Lic Chan, Chia-Min Chung, Youjin Deng, Michel Ferrero, Thomas M. Henderson, Carlos A. Jiménez-Hoyos, E. Kozik, Xuan-Wen Liu, Andrew J. Millis, N. V. Prokof’ev, Mingpu Qin, Gustavo E. Scuseria, Hao Shi, B. V. Svistunov, Luca F. Tocchio, I. S. Tupitsyn, Steven R. White, Shiwei Zhang, Bo-Xiao Zheng, Zhenyue Zhu, and Emanuel Gull, “Solutions of the Two-Dimensional Hubbard Model: Benchmarks and Results from a Wide Range of Numerical Algorithms,” *Phys. Rev. X* **5**, 041041 (2015).
- <sup>50</sup> Mingpu Qin, Hao Shi, and Shiwei Zhang, “Benchmark study of the two-dimensional Hubbard model with auxiliary-field quantum Monte Carlo method,” *Phys. Rev. B* **94**, 085103 (2016).
- <sup>51</sup> Chia-Chen Chang, Brenda M Rubenstein, and Miguel A Morales, “Auxiliary-field-based trial wave functions in quantum monte carlo calculations,” *Phys. Rev. B* **94**, 235144 (2016).
- <sup>52</sup> Bo-Xiao Zheng, Chia-Min Chung, Philippe Corboz, Georg Ehlers, Ming-Pu Qin, Reinhard M. Noack, Hao Shi, Steven R. White, Shiwei Zhang, and Garnet Kin-Lic Chan, “Stripe order in the underdoped region of the two-dimensional Hubbard model,” *Science* **358**, 1155–1160 (2017).
- <sup>53</sup> Mingpu Qin, Hao Shi, and Shiwei Zhang, “Numerical results on the short-range spin correlation functions in the ground state of the two-dimensional Hubbard model,” *Phys. Rev. B* **96**, 075156 (2017).
- <sup>54</sup> Peter Rosenberg, Hao Shi, and Shiwei Zhang, “Ultracold Atoms in a Square Lattice with Spin-Orbit Coupling: Charge Order, Superfluidity, and Topological Signatures,” *Phys. Rev. Lett.* **119**, 265301 (2017).
- <sup>55</sup> Adam Chiciak, Ettore Vitali, Hao Shi, and Shiwei Zhang, “Magnetic orders in the hole-doped three-band Hubbard model: Spin spirals, nematicity, and ferromagnetic domain walls,” *Phys. Rev. B* **97**, 235127 (2018).
- <sup>56</sup> Ettore Vitali, Hao Shi, Adam Chiciak, and Shiwei Zhang, “Metal-insulator transition in the ground state of the

- three-band Hubbard model at half filling,” *Phys. Rev. B* **99**, 165116 (2019).
- <sup>57</sup> The Simons Collaboration on the Many-Electron Problem, Chia-Min Chung, Mingpu Qin, Shiwei Zhang, Ulrich Schollwöck, and Steven R. White, “Plaquette versus ordinary  $d$ -wave pairing in the  $t$ -Hubbard model on a width-4 cylinder,” *Phys. Rev. B* **102**, 041106 (2020).
- <sup>58</sup> Simons Collaboration on the Many-Electron Problem, Mingpu Qin, Chia-Min Chung, Hao Shi, Ettore Vitali, Claudius Hubig, Ulrich Schollwöck, Steven R. White, and Shiwei Zhang, “Absence of Superconductivity in the Pure Two-Dimensional Hubbard Model,” *Phys. Rev. X* **10**, 031016 (2020).
- <sup>59</sup> Adam Chiciak, Ettore Vitali, and Shiwei Zhang, “Magnetic and charge orders in the ground state of the Emery model: Accurate numerical results,” *Phys. Rev. B* **102**, 214512 (2020).
- <sup>60</sup> Hao Xu, Hao Shi, Ettore Vitali, Mingpu Qin, and Shiwei Zhang, “Stripes and spin-density waves in the doped two-dimensional Hubbard model: Ground state phase diagram,” *Phys. Rev. Res.* **4**, 013239 (2022).
- <sup>61</sup> Ettore Vitali, Peter Rosenber, and Shiwei Zhang, “Exotic Superfluid Phases in Spin-Polarized Fermi Gases in Optical Lattices,” *Phys. Rev. Lett.* **128**, 203201 (2022).
- <sup>62</sup> Wirawan Purwanto and Shiwei Zhang, “Quantum Monte Carlo method for the ground state of many-boson systems,” *Phys. Rev. E* **70**, 056702 (2004).
- <sup>63</sup> Wirawan Purwanto and Shiwei Zhang, “Correlation effects in the ground state of trapped atomic Bose gases,” *Phys. Rev. A* **72**, 053610 (2005).
- <sup>64</sup> Brenda M. Rubenstein, Shiwei Zhang, and David R. Reichman, “Finite-temperature auxiliary-field quantum Monte Carlo technique for Bose-Fermi mixtures,” *Phys. Rev. A* **86**, 053606 (2012).
- <sup>65</sup> Joonho Lee, Shiwei Zhang, and David R. Reichman, “Constrained-path auxiliary-field quantum Monte Carlo for coupled electrons and phonons,” *Phys. Rev. B* **103**, 115123 (2021).
- <sup>66</sup> Shiwei Zhang and Henry Krakauer, “Quantum Monte Carlo Method using Phase-Free Random Walks with Slater Determinants,” *Phys. Rev. Lett.* **90**, 136401 (2003).
- <sup>67</sup> Wirawan Purwanto, Henry Krakauer, and Shiwei Zhang, “Pressure-induced diamond to  $\beta$ -tin transition in bulk silicon: A quantum monte carlo study,” *Phys. Rev. B* **80**, 214116 (2009).
- <sup>68</sup> Fengjie Ma, Wirawan Purwanto, Shiwei Zhang, and Henry Krakauer, “Quantum monte carlo calculations in solids with downfolded hamiltonians,” *Phys. Rev. Letters* **114**, 226401 (2015).
- <sup>69</sup> Mario Motta, David M Ceperley, Garnet Kin-Lic Chan, John A Gomez, Emanuel Gull, Sheng Guo, Carlos A Jiménez-Hoyos, Tran Nguyen Lan, Jia Li, Fengjie Ma, *et al.*, “Towards the solution of the many-electron problem in real materials: Equation of state of the hydrogen chain with state-of-the-art many-body methods,” *Phys. Rev. X* **7**, 031059 (2017).
- <sup>70</sup> Fengjie Ma, Shiwei Zhang, and Henry Krakauer, “Auxiliary-field quantum monte carlo calculations with multiple-projector pseudopotentials,” *Phys. Rev. B* **95**, 165103 (2017).
- <sup>71</sup> Shuai Zhang, Fionn D. Malone, and Miguel A. Morales, “Auxiliary-field quantum Monte Carlo calculations of the structural properties of nickel oxide,” *J. Chem. Phys.* **149**, 164102 (2018).
- <sup>72</sup> Brandon Eskridge, Henry Krakauer, and Shiwei Zhang, “Local Embedding and Effective Downfolding in the Auxiliary-Field Quantum Monte Carlo Method,” *J. Chem. Theory Comput.* **15**, 3949–3959 (2019).
- <sup>73</sup> Joonho Lee, Fionn D. Malone, and Miguel A. Morales, “An auxiliary-field quantum Monte Carlo perspective on the ground state of the dense uniform electron gas: An investigation with Hartree-Fock trial wavefunctions,” *J. Chem. Phys.* **151**, 064122 (2019).
- <sup>74</sup> Mario Motta, Shiwei Zhang, and Garnet Kin-Lic Chan, “Hamiltonian symmetries in auxiliary-field quantum monte carlo calculations for electronic structure,” *Phys. Rev. B* **100**, 045127 (2019).
- <sup>75</sup> Mario Motta, Claudio Genovese, Fengjie Ma, Zhi-Hao Cui, Randy Sawaya, Garnet Kin-Lic Chan, Natalia Chepiga, Phillip Helms, Carlos Jiménez-Hoyos, Andrew J Millis, *et al.*, “Ground-state properties of the hydrogen chain: dimerization, insulator-to-metal transition, and magnetic phases,” *Phys. Rev. X* **10**, 031058 (2020).
- <sup>76</sup> Fionn D. Malone, Shuai Zhang, and Miguel A. Morales, “Accelerating Auxiliary-Field Quantum Monte Carlo Simulations of Solids with Graphical Processing Units,” *J. Chem. Theory Comput.* **16**, 4286–4297 (2020).
- <sup>77</sup> Miguel A. Morales and Fionn D. Malone, “Accelerating the convergence of auxiliary-field quantum Monte Carlo in solids with optimized Gaussian basis sets,” *J. Chem. Phys.* **153**, 194111 (2020).
- <sup>78</sup> Fionn D Malone, Anouar Benali, Miguel A Morales, Michel Caffarel, Paul RC Kent, and Luke Shulenburg, “Systematic comparison and cross-validation of fixed-node diffusion monte carlo and phaseless auxiliary-field quantum monte carlo in solids,” *Phys. Rev. B* **102**, 161104 (2020).
- <sup>79</sup> Siyuan Chen, Mario Motta, Fengjie Ma, and Shiwei Zhang, “Ab initio electronic density in solids by many-body plane-wave auxiliary-field quantum monte carlo calculations,” *Phys. Rev. B* **103**, 075138 (2021).
- <sup>80</sup> Joonho Lee, Fionn D. Malone, Miguel A. Morales, and David R. Reichman, “Spectral Functions from Auxiliary-Field Quantum Monte Carlo without Analytic Continuation: The Extended Koopmans’ Theorem Approach,” *J. Chem. Theory Comput.* **17**, 3372–3387 (2021).
- <sup>81</sup> P. R. C. Kent, Abdulgani Annaberdiyev, Anouar Benali, M. Chandler Bennett, Edgar Josué Landinez Borda, Peter Doak, Hongxia Hao, Kenneth D. Jordan, Jaron T. Krogel, Ilkka Kylänpää, Joonho Lee, Ye Luo, Fionn D. Malone, Cody A. Melton, Lubos Mitas, Miguel A. Morales, Eric Neuscamman, Fernando A. Reboredo, Brenda Rubenstein, Kayahan Saritas, Shiv Upadhyay, Guangming Wang, Shuai Zhang, and Luning Zhao, “QMCPACK: Advances in the development, efficiency, and application of auxiliary field and real-space variational and diffusion quantum Monte Carlo,” *J. Chem. Phys.* **152**, 174105 (2020).
- <sup>82</sup> See <https://github.com/linusjoonho/ipie> for details on how to obtain the source code.
- <sup>83</sup> Fionn D. Malone, Ankit Mahajan, James S. Spencer, and Joonho Lee, “ipie: A Python-based Auxiliary-Field Quantum Monte Carlo Program with Flexibility and Efficiency on CPUs and GPUs,” *arXiv* (2022), 10.48550/arXiv.2209.04015, 2209.04015.
- <sup>84</sup> Krishnan Raghavachari, Gary W. Trucks, John A. Pople, and Martin Head-Gordon, “A fifth-order perturbation

- comparison of electron correlation theories,” *Chem. Phys. Lett.* **157**, 479–483 (1989).
- <sup>85</sup> Amir Karton, Shauli Daon, and Jan M.L. Martin, “W4-11: A high-confidence benchmark dataset for computational thermochemistry derived from first-principles w4 data,” *Chem. Phys. Lett.* **510**, 165–178 (2011).
- <sup>86</sup> Jan Rezáč and Pavel Hobza, “Describing noncovalent interactions beyond the common approximations: How accurate is the “gold standard,” ccsd (t) at the complete basis set limit?” *J. Chem. Theory Comput* **9**, 2151–2155 (2013).
- <sup>87</sup> K. Jankowski and J. Paldus, “Applicability of coupled-pair theories to quasidegenerate electronic states: A model study,” *Int. J. Quantum Chem.* **18**, 1243–1269 (1980).
- <sup>88</sup> Per E. M. Siegbahn, “The externally contracted CI method applied to N<sub>2</sub>,” *Int. J. Quantum Chem.* **23**, 1869–1889 (1983).
- <sup>89</sup> J Paldus, P Piecuch, L Pylypow, and B Jeziorski, “Application of hilbert-space coupled-cluster theory to simple (h 2) 2 model systems: Planar models,” *Phys. Rev. A* **47**, 2738 (1993).
- <sup>90</sup> Uttam Sinha Mahapatra, Barnali Datta, and Debashis Mukherjee, “A size-consistent state-specific multireference coupled cluster theory: Formal developments and molecular applications,” *J. Chem. Phys.* **110**, 6171–6188 (1999).
- <sup>91</sup> Karol Kowalski and Piotr Piecuch, “Complete set of solutions of multireference coupled-cluster equations: The state-universal formalism,” *Phys. Rev. A* **61**, 052506 (2000).
- <sup>92</sup> Francesco A. Evangelista, Wesley D. Allen, and Henry F. Schaefer, “High-order excitations in state-universal and state-specific multireference coupled cluster theories: Model systems,” *J. Chem. Phys.* **125**, 154113 (2006).
- <sup>93</sup> Jing Ma, Shuhua Li, and Wei Li, “A multireference configuration interaction method based on the separated electron pair wave functions,” *J. Comput. Chem.* **27**, 39–47 (2006).
- <sup>94</sup> David W. Small and Martin Head-Gordon, “A fusion of the closed-shell coupled cluster singles and doubles method and valence-bond theory for bond breaking,” *J. Chem. Phys.* **137**, 114103 (2012).
- <sup>95</sup> Joonho Lee, William J. Huggins, Martin Head-Gordon, and K. Birgitta Whaley, “Generalized Unitary Coupled Cluster Wave functions for Quantum Computation,” *J. Chem. Theory Comput.* **15**, 311–324 (2019).
- <sup>96</sup> S. E. Koonin, G. Sugiyama, H. Friedrichl, and W. K. Kellogg, “Auxiliary-Field Quantum Monte Carlo for Correlated Electron Systems,” in *Emergent Phenomena in Correlated Matter: Autumn School organized by the Forschungszentrum Jülich and the German Research School for Simulation Jülich 23 – 27 September 2013* (Forschungszentrum Jülich, 2013) p. 15.1.
- <sup>97</sup> Mario Motta and Shiwei Zhang, “Ab initio computations of molecular systems by the auxiliary-field quantum Monte Carlo method,” *WIREs Comput. Mol. Sci.* **8**, e1364 (2018).
- <sup>98</sup> Hao Shi and Shiwei Zhang, “Some recent developments in auxiliary-field quantum Monte Carlo for real materials,” *J. Chem. Phys.* **154**, 024107 (2021).
- <sup>99</sup> Hiroshi Nakatsuji, “Equation for the direct determination of the density matrix,” *Phys. Rev. A* **14**, 41 (1976).
- <sup>100</sup> Marcel Nooijen, “Can the eigenstates of a many-body hamiltonian be represented exactly using a general two-body cluster expansion?” *Phys. Rev. letters* **84**, 2108 (2000).
- <sup>101</sup> H. F. Trotter, “On the Product of Semi-Groups of Operators on JSTOR,” *Proc. Amer. Math. Soc.* **10**, 545–551 (1959).
- <sup>102</sup> J. Hubbard, “Calculation of partition functions,” *Phys. Rev. Lett.* **3**, 77 (1959).
- <sup>103</sup> J. Carlson, J. E. Gubernatis, G. Ortiz, and Shiwei Zhang, “Issues and observations on applications of the constrained-path monte carlo method to many-fermion systems,” *Phys. Rev. B* **59**, 12788 (1999).
- <sup>104</sup> Joonho Lee and Martin Head-Gordon, “Distinguishing artificial and essential symmetry breaking in a single determinant: approach and application to the C60, C36, and C20 fullerenes,” *Phys. Chem. Chem. Phys.* **21**, 4763–4778 (2019).
- <sup>105</sup> Leslie Farnell, John A. Pople, and Leo Radom, “Structural predictions for open-shell systems: a comparative assessment of ab initio procedures,” *J. Phys. Chem.* **87**, 79–82 (1983).
- <sup>106</sup> Ross H. Nobes, John A. Pople, Leo Radom, Nicholas C. Handy, and Peter J. Knowles, “Slow convergence of the møller-plesset perturbation series: the dissociation energy of hydrogen cyanide and the electron affinity of the cyano radical,” *Chem. Phys. Lett.* **138**, 481–485 (1987).
- <sup>107</sup> Peter M. W. Gill, John A. Pople, Leo Radom, and Ross H. Nobes, “Why does unrestricted Møller-Plesset perturbation theory converge so slowly for spin-contaminated wave functions?” *J. Chem. Phys.* **89**, 7307–7314 (1988).
- <sup>108</sup> Frank Jensen, “A remarkable large effect of spin contamination on calculated vibrational frequencies,” *Chem. Phys. Lett.* **169**, 519–528 (1990).
- <sup>109</sup> Jamie S. Andrews, Dylan Jayatilaka, Richard G.A. Bone, Nicholas C. Handy, and Roger D. Amos, “Spin contamination in single-determinant wavefunctions,” *Chem. Phys. Lett.* **183**, 423–431 (1991).
- <sup>110</sup> S. Yamanaka, M. Okumura, M. Nakano, and K. Yamaguchi, “EHF theory of chemical reactions Part 4. UNO CASSCF, UNO CASPT2 and R(U)HF coupled-cluster (CC) wavefunctions,” *J. Mol. Struct.* **310**, 205–218 (1994).
- <sup>111</sup> Philippe Y. Ayala and H. Bernhard Schlegel, “A nonorthogonal CI treatment of symmetry breaking in sigma formylxyl radical,” *J. Chem. Phys.* **108**, 7560 (1998).
- <sup>112</sup> T. Daniel Crawford and John F. Stanton, “Some surprising failures of Brueckner coupled cluster theory,” *J. Chem. Phys.* **112**, 7873 (2000).
- <sup>113</sup> Joonho Lee and Martin Head-Gordon, “Regularized Orbital-Optimized Second-Order Møller–Plesset Perturbation Theory: A Reliable Fifth-Order-Scaling Electron Correlation Model with Orbital Energy Dependent Regularizers,” *J. Chem. Theory Comput.* **14**, 5203–5219 (2018).
- <sup>114</sup> Clifford E. Dykstra, “An examination of the Brueckner condition for the selection of molecular orbitals in correlated wavefunctions,” *Chem. Phys. Lett.* **45**, 466–469 (1977).
- <sup>115</sup> Krishnan Raghavachari, John A. Pople, Eric S. Replogle, Martin Head-Gordon, and Nicholas C. Handy, “Size-consistent Brueckner theory limited to double and triple

- substitutions,” *Chem. Phys. Lett.* **167**, 115–121 (1990).
- <sup>116</sup> Mingpu Qin, Hao Shi, and Shiwei Zhang, “Coupling quantum monte carlo and independent-particle calculations: Self-consistent constraint for the sign problem based on the density or the density matrix,” *Phys. Rev. B* **94**, 235119 (2016).
- <sup>117</sup> Adam A. Holmes, Norm M. Tubman, and C. J. Umrigar, “Heat-Bath Configuration Interaction: An Efficient Selected Configuration Interaction Algorithm Inspired by Heat-Bath Sampling,” *J. Chem. Theory Comput.* **12**, 3674–3680 (2016).
- <sup>118</sup> R Hlubina, Sandro Sorella, and F Guinea, “Ferromagnetism in the two dimensional t-t’ hubbard model at the van hove density,” *Phys. Rev. Letters* **78**, 1343 (1997).
- <sup>119</sup> William J. Huggins, Bryan A. O’Gorman, Nicholas C. Rubin, David R. Reichman, Ryan Babbush, and Joonho Lee, “Unbiasing fermionic quantum Monte Carlo with a quantum computer,” *Nature* **603**, 416–420 (2022).
- <sup>120</sup> William A. Goddard, Thom H. Dunning, William J. Hunt, and P. Jeffrey Hay, “Generalized valence bond description of bonding in low-lying states of molecules,” *Acc. Chem. Res.* **6**, 368–376 (1973).
- <sup>121</sup> Thomas Schraivogel, Aron J. Cohen, Ali Alavi, and Daniel Kats, “Transcorrelated coupled cluster methods,” *J. Chem. Phys.* **155**, 191101 (2021).
- <sup>122</sup> Rodney J. Bartlett and Jozef Noga, “The expectation value coupled-cluster method and analytical energy derivatives,” *Chem. Phys. Lett.* **150**, 29–36 (1988).
- <sup>123</sup> Thomas Bondo Pedersen and Henrik Koch, “Coupled cluster response functions revisited,” *J. Chem. Phys.* **106**, 8059–8072 (1997).
- <sup>124</sup> PA Whitlock, DM Ceperley, GV Chester, and MH Kalos, “Properties of liquid and solid he 4,” *Phys. Rev. B* **19**, 5598 (1979).
- <sup>125</sup> M. RothsteinStuart, “A survey on pure sampling in quantum Monte Carlo methods,” *Can. J. Chem.* (2013).
- <sup>126</sup> Shiwei Zhang, Joseph Carlson, and James E Gubernatis, “Constrained path monte carlo method for fermion ground states,” *Physical Review B* **55**, 7464 (1997).
- <sup>127</sup> R. J. Bartlett, “Many-Body Perturbation Theory and Coupled Cluster Theory for Electron Correlation in Molecules,” *Annu. Rev. Phys. Chem.* **32**, 359–401 (1981).
- <sup>128</sup> Lars Goerigk, Andreas Hansen, Christoph Bauer, Stephan Ehrlich, Asim Najibi, and Stefan Grimme, “A look at the density functional theory zoo with the advanced GMTKN55 database for general main group thermochemistry, kinetics and noncovalent interactions,” *Phys. Chem. Chem. Phys.* **19**, 32184–32215 (2017).
- <sup>129</sup> J. Weber, David R. Reichman, Richard A. Friesner, and Shiwei Zhang, “unpublished,” (2022).
- <sup>130</sup> “Data repository for “twenty years of auxiliary-field quantum monte carlo in quantum chemistry: An overview and assessment on main group chemistry and bond-breaking”,” (2022).
- <sup>131</sup> Narbe Mardirossian and Martin Head-Gordon, “ $\omega$ B97M-V: A combinatorially optimized, range-separated hybrid, meta-GGA density functional with VV10 nonlocal correlation,” *J. Chem. Phys.* **144**, 214110 (2016).
- <sup>132</sup> Narbe Mardirossian and Martin Head-Gordon, “Survival of the most transferable at the top of Jacob’s ladder: Defining and testing the  $\omega$ B97M(2) double hybrid density functional,” *J. Chem. Phys.* **148**, 241736 (2018).
- <sup>133</sup> Jan M. L. Martin and Golokesh Santra, “Empirical Double-Hybrid Density Functional Theory: A ‘Third Way’ in Between WFT and DFT,” *Isr. J. Chem.* **60**, 787–804 (2020).
- <sup>134</sup> Yasmine S. Al-Hamdani, Péter R. Nagy, Andrea Zen, Dennis Barton, Mihály Kállay, Jan Gerit Brandenburg, and Alexandre Tkatchenko, “Interactions between large molecules pose a puzzle for reference quantum mechanical methods,” *Nat. Commun.* **12**, 1–12 (2021).
- <sup>135</sup> Joonho Lee, David W. Small, Evgeny Epifanovsky, and Martin Head-Gordon, “Coupled-Cluster Valence-Bond Singles and Doubles for Strongly Correlated Systems: Block-Tensor Based Implementation and Application to Oligoacenes,” *J. Chem. Theory Comput.* **13**, 602–615 (2017).
- <sup>136</sup> Kerstin. Andersson, Per Aake. Malmqvist, Bjoern O. Roos, Andrzej J. Sadlej, and Krzysztof. Wolinski, “Second-order perturbation theory with a CASSCF reference function,” *J. Phys. Chem.* **94**, 5483–5488 (1990).
- <sup>137</sup> Kerstin Andersson, Per-Åke Malmqvist, and Björn O. Roos, “Second-order perturbation theory with a complete active space self-consistent field reference function,” *J. Chem. Phys.* **96**, 1218–1226 (1992).
- <sup>138</sup> C. Angeli, R. Cimiraglia, S. Evangelisti, T. Leininger, and J.-P. Malrieu, “Introduction of n-electron valence states for multireference perturbation theory,” *J. Chem. Phys.* **114**, 10252–10264 (2001).
- <sup>139</sup> Celestino Angeli, Renzo Cimiraglia, and Jean-Paul Malrieu, “n-electron valence state perturbation theory: A spinless formulation and an efficient implementation of the strongly contracted and of the partially contracted variants,” *J. Chem. Phys.* **117**, 9138–9153 (2002).
- <sup>140</sup> K. Hirao, “Multireference Møller—Plesset method,” *Chem. Phys. Lett.* **190**, 374–380 (1992).
- <sup>141</sup> Robert J. Gdanitz and Reinhart Ahlrichs, “The averaged coupled-pair functional (ACPF): A size-extensive modification of MR CI(SD),” *Chem. Phys. Lett.* **143**, 413–420 (1988).
- <sup>142</sup> Péter G. Szalay and Rodney J. Bartlett, “Multi-reference averaged quadratic coupled-cluster method: a size-extensive modification of multi-reference CI,” *Chem. Phys. Lett.* **214**, 481–488 (1993).
- <sup>143</sup> Péter G. Szalay and Rodney J. Bartlett, “Approximately extensive modifications of the multireference configuration interaction method: A theoretical and practical analysis,” *J. Chem. Phys.* **103**, 3600–3612 (1995).
- <sup>144</sup> Pablo J. Bruna, Sigrid D. Peyerimhoff, and Robert J. Buenker, “The ground state of the CN+ ion: a multi-reference Ci study,” *Chem. Phys. Lett.* **72**, 278–284 (1980).
- <sup>145</sup> Peter G. Burton, Robert J. Buenker, Pablo J. Bruna, and Sigrid D. Peyerimhoff, “Comparison of perturbatively corrected MRD CI results with a full CI treatment of the BH ground state,” *Chem. Phys. Lett.* **95**, 379–385 (1983).
- <sup>146</sup> Chenyang Li and Francesco A. Evangelista, “Multireference Driven Similarity Renormalization Group: A Second-Order Perturbative Analysis,” *J. Chem. Theory Comput.* **11**, 2097–2108 (2015).
- <sup>147</sup> Chenyang Li and Francesco A. Evangelista, “Driven similarity renormalization group: Third-order multireference perturbation theory,” *J. Chem. Phys.* **146**, 124132 (2017).
- <sup>148</sup> Chenyang Li and Francesco A. Evangelista, “Towards numerically robust multireference theories: The driven similarity renormalization group truncated to one- and two-body operators,” *J. Chem. Phys.* **144**, 164114 (2016).

- <sup>149</sup> Björn O. Roos and Kerstin Andersson, “Multiconfigurational perturbation theory with level shift — the Cr<sub>2</sub> potential revisited,” *Chem. Phys. Lett.* **245**, 215–223 (1995).
- <sup>150</sup> Björn O. Roos, Kerstin Andersson, Markus P. Fülcher, Luis Serrano-Andrés, Kristine Pierloot, Manuela Merchán, and Vicent Molina, “Applications of level shift corrected perturbation theory in electronic spectroscopy,” *J. Mol. Struct. THEOCHEM* **388**, 257–276 (1996).
- <sup>151</sup> Niclas Forsberg and Per-Åke Malmqvist, “Multiconfiguration perturbation theory with imaginary level shift,” *Chem. Phys. Lett.* **274**, 196–204 (1997).
- <sup>152</sup> Giovanni Ghigo, Björn O. Roos, and Per-Åke Malmqvist, “A modified definition of the zeroth-order Hamiltonian in multiconfigurational perturbation theory (CASPT2),” *Chem. Phys. Lett.* **396**, 142–149 (2004).
- <sup>153</sup> Fionn D. Malone, Anouar Benali, Miguel A. Morales, Michel Caffarel, Paul R. C. Kent, and Luke Shulenburg, “Systematic comparison and cross-validation of fixed-node diffusion Monte Carlo and phaseless auxiliary-field quantum Monte Carlo in solids,” *Phys. Rev. B* **102**, 161104 (2020).
- <sup>154</sup> Joonho Lee and Martin Head-Gordon, “Two single-reference approaches to singlet biradicaloid problems: Complex, restricted orbitals and approximate spin-projection combined with regularized orbital-optimized Møller-Plesset perturbation theory,” *J. Chem. Phys.* **150**, 244106 (2019).
- <sup>155</sup> Nelson H.F. Beebe and Jan Lindenberg, “Simplifications in the generation and transformation of two-electron integrals in molecular calculations,” *Int. J. Quantum Chem.* **12**, 683–705 (1977).
- <sup>156</sup> Francesco Aquilante, Luca De Vico, Nicolas Ferré, Giovanni Ghigo, Per-Åke Malmqvist, Pavel Neogrády, Thomas Bondo Pedersen, Michal Pitoňák, Markus Reiher, Björn O. Roos, Luis Serrano-Andrés, Miroslav Urban, Valera Veryazov, and Roland Lindh, “Molcas 7: the next generation,” *J. Comput. Chem.* **31**, 224–247 (2010).
- <sup>157</sup> B. I. Dunlap, J. W.D. Connolly, and J. R. Sabin, “On some approximations in applications of X $\alpha$  theory,” *J. Chem. Phys.* **71**, 3396–3402 (1979).
- <sup>158</sup> Florian Weigend, Andreas Köhn, and Christof Hättig, “Efficient use of the correlation consistent basis sets in resolution of the identity MP2 calculations,” *J. Chem. Phys.* **116**, 3175–3183 (2002).
- <sup>159</sup> D. J. Thouless, “Stability conditions and nuclear rotations in the Hartree-Fock theory,” *Nuc. Phys.* **21**, 225 (1960).
- <sup>160</sup> D. J. Thouless, “Vibrational states of nuclei in the random phase approximation,” *Nuc. Phys.* **22**, 78 (1961).
- <sup>161</sup> Thom H. Dunning, “Gaussian basis sets for use in correlated molecular calculations. I. The atoms boron through neon and hydrogen,” *J. Chem. Phys.* **90**, 1007–1023 (1989).
- <sup>162</sup> Lucas K. Wagner, Michal Bajdich, and Lubos Mitas, “Qwalk: A quantum monte carlo program for electronic structure,” *J. Comput. Phys.* **228**, 3390 (2009).
- <sup>163</sup> Trygve Helgaker, Wim Klopper, Henrik Koch, and Jozef Noga, “Basis-set convergence of correlated calculations on water,” *J. Chem. Phys.* **106**, 9639–9646 (1997).
- <sup>164</sup> Qiming Sun, Xing Zhang, Samragni Banerjee, Peng Bao, Marc Barbry, Nick S. Blunt, Nikolay A. Bogdanov, George H. Booth, Jia Chen, Zhi-Hao Cui, Janus J. Eriksen, Yang Gao, Sheng Guo, Jan Hermann, Matthew R. Hermes, Kevin Koh, Peter Koval, Susi Lehtola, Zhen-dong Li, Junzi Liu, Narbe Mardirossian, James D. McClain, Mario Motta, Bastien Mussard, Hung Q. Pham, Artem Pulkin, Wirawan Purwanto, Paul J. Robinson, Enrico Ronca, Elvira R. Sayfutyarova, Maximilian Scheurer, Henry F. Schurkus, James E. T. Smith, Chong Sun, Shi-Ning Sun, Shiv Upadhyay, Lucas K. Wagner, Xiao Wang, Alec White, James Daniel Whitfield, Mark J. Williamson, Sebastian Wouters, Jun Yang, Jason M. Yu, Tianyu Zhu, Timothy C. Berkelbach, Sandeep Sharma, Alexander Yu. Sokolov, and Garnet Kin-Lic Chan, “Recent developments in the PySCF program package,” *J. Chem. Phys.* **153**, 024109 (2020).
- <sup>165</sup> Evgeny Epifanovsky, Andrew T. B. Gilbert, Xintian Feng, Joonho Lee, Yuezhi Mao, Narbe Mardirossian, Pavel Pokhilko, Alec F. White, Marc P. Coons, Adrian L. Dempwolff, Zhengting Gan, Diptarka Hait, Paul R. Horn, Leif D. Jacobson, Ilya Kaliman, Jörg Kussmann, Adrian W. Lange, Ka Un Lao, Daniel S. Levine, Jie Liu, Simon C. McKenzie, Adrian F. Morrison, Kaushik D. Nanda, Felix Plasser, Dirk R. Rehn, Marta L. Vidal, Zhi-Qiang You, Ying Zhu, Bushra Alam, Benjamin J. Albrecht, Abdulrahman Aldossary, Ethan Alguire, Josefine H. Andersen, Vishikh Athavale, Dennis Barton, Khadiza Begam, Andrew Behn, Nicole Bellonzi, Yves A. Bernard, Eric J. Berquist, Hugh G. A. Burton, Abel Carreras, Kevin Carter-Fenk, Romit Chakraborty, Alan D. Chien, Kristina D. Closser, Vale Cofer-Shabica, Saswata Dasgupta, Marc de Wergifosse, Jia Deng, Michael Diedenhofen, Hainam Do, Sebastian Ehlert, Po-Tung Fang, Shervin Fatehi, Qingguo Feng, Triet Friedhoff, James Gayvert, Qinghui Ge, Gergely Gidofalvi, Matthew Goldey, Joe Gomes, Cristina E. González-Espinoza, Sahil Gulania, Anastasia O. Gunina, Magnus W. D. Hanson-Heine, Phillip H. P. Harbach, Andreas Hauser, Michael F. Herbst, Mario Hernández Vera, Manuel Hodecker, Zachary C. Holden, Shannon Houck, Xunkun Huang, Kerwin Hui, Bang C. Huynh, Maxim Ivanov, Ádám Jász, Hyunjun Ji, Hanjie Jiang, Benjamin Kaduk, Sven Kähler, Kirill Khistyayev, Jaehoon Kim, Gergely Kis, Phil Klunzinger, Zsuzsanna Koczor-Benda, Joong Hoon Koh, Dimitri Kosenkov, Laura Koulias, Tim Kowalczyk, Caroline M. Krauter, Karl Kue, Alexander Kunitsa, Thomas Kus, István Ladjászki, Arie Landau, Keith V. Lawler, Daniel Lefrancois, Susi Lehtola, Run R. Li, Yi-Pei Li, Jiashu Liang, Marcus Liebenthal, Hung-Hsuan Lin, You-Sheng Lin, Fenglai Liu, Kuan-Yu Liu, Matthias Loipersberger, Arne Luenser, Aaditya Manjanath, Prashant Manohar, Erum Mansoor, Sam F. Manzer, Shan-Ping Mao, Aleksandr V. Marenich, Thomas Markovich, Stephen Mason, Simon A. Maurer, Peter F. McLaughlin, Maximilian F. S. J. Menger, Jan-Michael Mewes, Stefanie A. Mewes, Pierpaolo Morgante, J. Wayne Mullinax, Katherine J. Oosterbaan, Garrette Paran, Alexander C. Paul, Suranjan K. Paul, Fabijan Pavošević, Zheng Pei, Stefan Prager, Emil I. Proynov, Ádám Rák, Eloy Ramos-Cordoba, Bhaskar Rana, Alan E. Rask, Adam Rettig, Ryan M. Richard, Fazle Rob, Elliot Rossomme, Tarek Scheele, Maximilian Scheurer, Matthias Schneider, Nikolai Sergueev, Shaama M. Sharada, Wojciech Skomorowski, David W. Small, Christopher J. Stein, Yu-Chuan Su, Eric J. Sundstrom, Zhen Tao, Jonathan Thirman, Gábor J. Tornai, Takashi Tsuchimochi, Norm M. Tubman, Srimukh Prasad Veccham, Oleg Vydrov, Jan Wenzel, Jon Witte, Atsushi Yamada, Kun Yao, Sina Yeganeh, Shane R. Yost, Alexander Zech,

- Igor Ying Zhang, Xing Zhang, Yu Zhang, Dmitry Zuev, Alán Aspuru-Guzik, Alexis T. Bell, Nicholas A. Besley, Ksenia B. Bravaya, Bernard R. Brooks, David Casanova, Jeng-Da Chai, Sonia Coriani, Christopher J. Cramer, György Cserey, A. Eugene DePrince, Robert A. DiStasio, Andreas Dreuw, Barry D. Dunietz, Thomas R. Furlani, William A. Goddard, Sharon Hammes-Schiffer, Teresa Head-Gordon, Warren J. Hehre, Chao-Ping Hsu, Thomas-C. Jagau, Yousung Jung, Andreas Klamt, Jing Kong, Daniel S. Lambrecht, WanZhen Liang, Nicholas J. Mayhall, C. William McCurdy, Jeffrey B. Neaton, Christian Ochsenfeld, John A. Parkhill, Roberto Peverati, Vitaly A. Rassolov, Yihan Shao, Lyudmila V. Slipchenko, Tim Stauch, Ryan P. Steele, Joseph E. Subotnik, Alex J. W. Thom, Alexandre Tkatchenko, Donald G. Truhlar, Troy Van Voorhis, Tomasz A. Wesolowski, K. Birgitta Whaley, H. Lee Woodcock, Paul M. Zimmerman, Shirin Faraji, Peter M. W. Gill, Martin Head-Gordon, John M. Herbert, and Anna I. Krylov, "Software for the frontiers of quantum chemistry: An overview of developments in the Q-Chem 5 package," *J. Chem. Phys.* **155**, 084801 (2021).
- <sup>166</sup> See <https://github.com/sanshar/Dice> for details on how to obtain the source code.
- <sup>167</sup> Frank Neese, "Software update: the ORCA program system, version 4.0," *WIREs Comput. Mol. Sci.* **8**, e1327 (2018).
- <sup>168</sup> Daniel G. A. Smith, Lori A. Burns, Andrew C. Simmonett, Robert M. Parrish, Matthew C. Schieber, Raimondas Galvelis, Peter Kraus, Holger Kruse, Roberto Di Remigio, Asem Alenaizan, Andrew M. James, Susi Lehtola, Jonathon P. Misiewicz, Maximilian Scheurer, Robert A. Shaw, Jeffrey B. Schriber, Yi Xie, Zachary L. Glick, Dominic A. Sirianni, Joseph Senan O'Brien, Jonathan M. Waldrop, Ashutosh Kumar, Edward G. Hohenstein, Benjamin P. Pritchard, Bernard R. Brooks, Henry F. Schaefer, Alexander Yu. Sokolov, Konrad Patkowski, A. Eugene DePrince, Uğur Bozkaya, Rollin A. King, Francesco A. Evangelista, Justin M. Turney, T. Daniel Crawford, and C. David Sherrill, "PSI4 1.4: Open-source software for high-throughput quantum chemistry," *J. Chem. Phys.* **152**, 184108 (2020).